



Norwegian University of  
Science and Technology

# Basis for estimation of heat and mass balance and CO<sub>2</sub> emissions in LNG plants

**Eduardo Fernández**

Natural Gas Technology

Submission date: December 2015

Supervisor: Jostein Pettersen, EPT

Norwegian University of Science and Technology  
Department of Energy and Process Engineering



EPT-M-2015-130

**MASTER THESIS**

for

Student Eduardo Fernandez Castro

Fall 2015

**Basis for estimation of heat and mass balance and CO<sub>2</sub> emissions in LNG plants***Basis for estimering av varme/massebalanse og CO<sub>2</sub>-utslipp i LNG-anlegg***Background and objective**

In early phases of an LNG project, or when considering the potential economy of a LNG development opportunity or gas discovery, simple calculations are often needed to assess key numbers such as production capacities (LNG, LPG, condensate), driver power needs, driver type, cooling method, utilities needs (heat, power), fuel gas use (“shrinkage”), and CO<sub>2</sub> emissions from feed gas and energy system. If possible, the model can also include estimates for gross calorific value of the LNG product. Such numbers provide an important basis for project assessment and economic analysis.

This type of data are often based on rough “scaling” of values from known installations or projects, with potential errors or unintended or unknown factors affecting the result, especially if site-specific parameters such as gas composition, climatic data and process type vary. Ideally, the estimates should be based on “first principles”, giving robustness and correctness in estimates.

The objective of the present work is therefore to establish the basis for an early-phase heat and mass balance model and CO<sub>2</sub> emission estimate model for LNG plant developments (onshore or floating/offshore). The basis should be established based on simplified process models and published information, covering a realistic range of data and possible plant configurations. Numbers can be benchmarked against known data from actual plants, or more detailed engineering information from LNG projects or studies.

**The following tasks are to be considered:**

1. Literature survey on published LNG plant information and prior published work on simplified heat/mass balance and CO<sub>2</sub> emissions from LNG production. The survey should also provide data that can be used for later model testing and benchmarking.
2. Establishment of model basis for estimating heat/mass balance of LNG production plants, based on relevant simplified configurations (block diagrams), using simplified and robust subsystem models. Results from process modelling software (Hysys or Pro/II) may provide basis for some of the simplified subsystem models.

3. Implementation of relevant models in a test version (e.g. spreadsheet) and testing of modelling results against LNG plant data.
4. Analysis and discussion of results and findings, including recommendations for further work.

Within 14 days of receiving the written text on the master thesis, the candidate shall submit a research plan for his project to the department.

When the thesis is evaluated, emphasis is put on processing of the results, and that they are presented in tabular and/or graphic form in a clear manner, and that they are analyzed carefully.

The thesis should be formulated as a research report with summary both in English and Norwegian, conclusion, literature references, table of contents etc. During the preparation of the text, the candidate should make an effort to produce a well-structured and easily readable report. In order to ease the evaluation of the thesis, it is important that the cross-references are correct. In the making of the report, strong emphasis should be placed on both a thorough discussion of the results and an orderly presentation.

The candidate is requested to initiate and keep close contact with his/her academic supervisor(s) throughout the working period. The candidate must follow the rules and regulations of NTNU as well as passive directions given by the Department of Energy and Process Engineering.

Risk assessment of the candidate's work shall be carried out according to the department's procedures. The risk assessment must be documented and included as part of the final report. Events related to the candidate's work adversely affecting the health, safety or security, must be documented and included as part of the final report. If the documentation on risk assessment represents a large number of pages, the full version is to be submitted electronically to the supervisor and an excerpt is included in the report.

Pursuant to "Regulations concerning the supplementary provisions to the technology study program/Master of Science" at NTNU §20, the Department reserves the permission to utilize all the results and data for teaching and research purposes as well as in future publications.

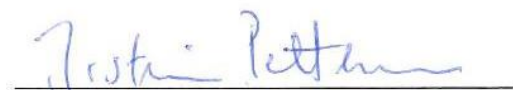
The final report is to be submitted digitally in DAIM. An executive summary of the thesis including title, student's name, supervisor's name, year, department name, and NTNU's logo and name, shall be submitted to the department as a separate pdf file. Based on an agreement with the supervisor, the final report and other material and documents may be given to the supervisor in digital format.

- Work to be done in lab (Water power lab, Fluids engineering lab, Thermal engineering lab)
- Field work

Department of Energy and Process Engineering, 25 August 2015



Olav Bolland  
Department Head



Jostein Pettersen  
Academic Supervisor

## PREFACE

This report has been written as the Master thesis of the MSc in Natural Gas Technology, at the Department of Energy and Process Engineering of the Norwegian University of Science and Technology (NTNU).

I would like to express my gratitude to Professor Jostein Pettersen, who has guided me on the project since the very first moment, from the provision of reference data to his personal suggestions that facilitated the creation of this work. I would also like to thank my entire family for their support from my home country. They have always encouraged me to do what I thought best, and my position at this time is thanks to their love. My gratitude also goes to Rubén Ensalsado, who taught me how to be and act as a real engineer. Finally, I would like to thank Paola Ivars, for her patience to bear with me and for her immeasurable help from the very first hour of every single day. Thank you for reminding me what really matters in life.



## ABSTRACT

The present work has been performed to provide initial estimations of the production rate, energy demand and CO<sub>2</sub> emissions in early phase LNG plant projects. The model created has been developed to be implemented in Microsoft Excel, and focus has been given to the definition of simple expressions that could be applied in the mentioned spreadsheet software. The model has been defined for an objective accuracy of +/- 30% with respect to the reference data. The plant model has been split into different blocks which represent different processes in the plant, and each block has been modelled differently by using HYSYS simulations, real data and theoretical models. Six reference cases have been benchmarked against the model estimations for the LNG, LPG and Condensate production, liquefaction power and CO<sub>2</sub> emissions from the feed gas and for the liquefaction power, electrical power and heat generation. Moreover, additional electrical power, heat duty and fuel gas flow rate estimations have been benchmarked against two of the reference cases. The representative estimations for the six reference cases present an accuracy range between -19% and +28%. The Condensate production estimation presents deviations between the reference and the predicted data outside of the +/-30% limit, and LPG production has been modelled for a single case with a deviation of -16%. Representative electrical power, heat duty and fuel flow rate estimations for cases A and B present relative error percentages between -10% and +25%.





**TABLE OF CONTENTS**

Preface .....	v
Abstract.....	vii
List of figures .....	xiii
List of tables .....	xvii
Nomenclature .....	xix
1 Introduction .....	1
1.1 Background .....	1
1.2 Report structure.....	1
2 Process description.....	3
2.1 LNG production plants .....	3
2.2 Location impact on the process.....	5
2.3 Product specifications and requirements.....	5
2.3.1 LNG plant products .....	5
2.3.2 LNG specifications .....	6
2.3.3 Condensate specifications.....	7
2.3.4 LPG specifications.....	7
3 Modelling basis and development.....	9
3.1 Modelling Software .....	9
3.1.1 Microsoft Excel .....	9
3.1.2 Aspen HYSYS.....	9
3.2 Objective parameters.....	10

3.3	Basis for LNG plant model .....	10
3.3.1	User inputs .....	11
3.3.2	Model layout .....	12
3.4	Block development .....	13
3.4.1	Process temperature definition .....	13
3.4.2	Separation .....	14
3.4.3	Gas Treatment Section.....	14
3.4.4	NGL Extraction .....	20
3.4.5	Liquefaction unit.....	24
3.4.6	End flash .....	29
3.4.7	Total power and heat duty calculations .....	31
3.4.8	Drivers .....	32
3.4.9	Fuel gas calculation .....	35
4	Model testing.....	37
4.1	Reference cases .....	37
4.2	Testing results for the six cases .....	39
4.2.1	Liquefaction power.....	39
4.2.2	LNG production.....	40
4.2.3	LPG production .....	41
4.2.4	Condensate production .....	42
4.2.5	CO <sub>2</sub> emissions from feed gas .....	42

4.2.6	CO <sub>2</sub> emission from liquefaction drivers, electrical power and heat generation..	43
4.2.7	Validation of the cases.....	44
4.3	Testing results for cases A and B.....	45
4.3.1	Total power and heat duty .....	45
4.3.2	MDEA solution pump and regenerator .....	46
4.3.3	Dehydration .....	47
4.3.4	De-ethanizer.....	47
4.3.5	Fuel gas flow rate .....	48
5	Conclusions and recommendations .....	51
6	References .....	53
	Appendix A: Condensate Stabilization model .....	55
	Appendix B: Gas Sweetening Unit calculations .....	57
	Appendix C: Dehydration Unit calculations .....	59
	Appendix D: NGL Extraction and Fractionation .....	61
	Appendix E: Liquefaction correction factors .....	63
	Appendix F: Upstream fuel gas intake .....	65
	Appendix G: Numerical test results .....	67
	Appendix H: Model implementation.....	69



## LIST OF FIGURES

<b>Figure 1.</b> Typical LNG plant flow diagram (adapted from [1]).	3
<b>Figure 2.</b> Examples of Gross Calorific Value ranges [3].	7
<b>Figure 3.</b> Simplified block diagram of the proposed model.	10
<b>Figure 4.</b> Process to create the model.	11
<b>Figure 5.</b> Principle sketch for the proposed model.	12
<b>Figure 6.</b> Solution pump power for different pressures as a function of the total CO <sub>2</sub> mass flow rate.	17
<b>Figure 7.</b> Specific pumping power variation depending on the feed gas pressure and temperature for a CO <sub>2</sub> content in the feed gas of 4 mol %.	17
<b>Figure 8.</b> Dehydration heat duty as a function of the total gas mass flow rate.	19
<b>Figure 9.</b> Graph representing the effect of the pressure and temperature on the heat duty. Each line represents the percentage variation of the head consumption depending on each parameter.	20
<b>Figure 10.</b> Flow diagram for the mass balance calculation in the NGL extraction unit.	21
<b>Figure 11.</b> Heat duty variation of the de-ethanizer reboiler depending on the feed gas temperature and pressure.	22
<b>Figure 12.</b> Specific heat duty of the de-ethanizer reboiler depending on the composition.	23
<b>Figure 13.</b> Graph representing the effect of the pressure, temperature and composition on the work consumption. Each line represents the percentage variation of the work consumption depending on each parameter.	28
<b>Figure 14.</b> Flow diagram for the N <sub>2</sub> Mass balance calculation.	29
<b>Figure 15.</b> Flash gas mass percentage relative to the total gas flow rate, as a function of the C <sub>1</sub> and N <sub>2</sub> in the liquefied gas.	30

<b>Figure 16.</b> LM6000 efficiency at different ambient temperature (adapted from [9]).	33
<b>Figure 17.</b> Frame 7 efficiency at different ambient temperature (adapted from [10]).	33
<b>Figure 18.</b> Typical fuel gas balance in LNG plants (source: BP).	35
<b>Figure 19.</b> Relative error percentage in liquefaction power for the six cases.	40
<b>Figure 20.</b> Relative error percentage in LNG production for the six cases.	41
<b>Figure 21.</b> Relative error in the LPG production for case B.	41
<b>Figure 22.</b> Relative error percentage in the Condensate production for the six cases.	42
<b>Figure 23.</b> Relative error percentage in the CO <sub>2</sub> emissions from feed for the six cases.	43
<b>Figure 24.</b> Relative error percentage in the CO <sub>2</sub> emissions from the liquefaction drivers, electrical power and heat generation for the six cases.	43
<b>Figure 25.</b> Results summary for the six different cases.	44
<b>Figure 26.</b> Relative error percentage in the Total electrical power and heat duty.	46
<b>Figure 27.</b> Relative error percentage in the MDEA solution regenerator and pump power model.	46
<b>Figure 28.</b> Relative error percentage in the dehydration heat duty model	47
<b>Figure 29.</b> Relative error percentage in the de-ethanizer heat duty model.	48
<b>Figure 30.</b> Relative error percentage in the fuel gas flow rate model.	49
<b>Figure 31.</b> Pressure-Temperature diagram of different pure components in the feed gas.	55
<b>Figure 32.</b> Variation of the heat duty for different mean components. The graph shows the relative variation with respect to the C <sub>8</sub> that was decided to be used as mean component.	56
<b>Figure 33.</b> Pumping power consumption as a function of the Amine mass flow rate and the feed gas inlet pressure.	57
<b>Figure 34.</b> Parameter “a” as a function of feed gas arrival pressure.	58

<b>Figure 35.</b> Variation of the heating load with the feed gas rate, temperature and pressure. ...	59
<b>Figure 36.</b> Parameter $\alpha$ as a function of the C2 mol % . .....	61
<b>Figure 37.</b> Parameter $\beta$ as a function of the C2 content. ....	62
<b>Figure 38.</b> Data curve approximations for the definition of $KP$ . ....	63
<b>Figure 39.</b> Data Curve approximations for the definition of $KT$ .....	64
<b>Figure 40.</b> Iterative algorithm used to calculate the fuel gas need. ....	65
<b>Figure 41.</b> Inputs sheet layout. ....	70
<b>Figure 42.</b> Gas Sweetening Unit sheet layout .....	71
<b>Figure 43.</b> Dehydration Unit sheet layout. ....	72
<b>Figure 44.</b> NGL Extraction model composition and presentation of the mass flow to liquefaction. ....	73
<b>Figure 45.</b> These tables present the split ratio contributing to the mass balance of the unit, and the energy balance in the de-ethanizer to obtain the heat duty of the NGL Extraction model.	74
<b>Figure 46.</b> Liquefaction Unit model layout. ....	75
<b>Figure 47.</b> End flash composition, GHV calculation and split ratio contributing to the mass balance of the model. ....	76
<b>Figure 48.</b> Driver model sheet layout and CO <sub>2</sub> emissions estimation from the liquefaction drivers, electrical power consumption and heat generation. ....	77
<b>Figure 49.</b> Results sheet summary presenting all the results estimated. ....	78





## LIST OF TABLES

<b>Table 1.</b> LNG component specifications. ....	6
<b>Table 2.</b> Condensate specifications. ....	7
<b>Table 3.</b> LPG component specifications. ....	7
<b>Table 4.</b> Main products obtained from the process. ....	10
<b>Table 5.</b> Definition of the feed gas parameters, ambient parameters, and number of yearly operation days. ....	11
<b>Table 6.</b> Plant parameters that require a technical decision for the plant estimations. ....	12
<b>Table 7.</b> Definition of the composition range of the liquefied gas components depending on the methane mol%. ....	21
<b>Table 8.</b> Definition of the gas entering the liquefaction unit for each richness classification. These split ratios are only applied when LPG is produced. ....	22
<b>Table 9.</b> Exergy efficiencies of the different process types. ....	26
<b>Table 10.</b> Reference compositions and KC definition depending on the gas richness. ....	27
<b>Table 11.</b> Specific power based on the reference conditions, for a medium gas richness. ....	28
<b>Table 12.</b> Definition of the efficiencies for each one of the power plants types, and scaling factor for estimation of the CO <sub>2</sub> emissions for each one. ....	34
<b>Table 13.</b> Main Plant parameters of the benchmarking cases. ....	37
<b>Table 14.</b> Main feed gas and process parameters of the benchmarking cases. ....	38
<b>Table 15.</b> Feed gas composition in mol percent of the benchmarking cases. ....	38
<b>Table 16.</b> Reference values for liquefaction power, mass balance and CO <sub>2</sub> emissions. ....	38
<b>Table 17.</b> Reference values for work and heat balance for cases A and B. ....	39
<b>Table 18.</b> Model results used for benchmarking of the six cases. ....	39

LIST OF TABLES

**Table 19.** Additional model results for the six cases. .... 45

**Table 20.** Numerical results for the comparison of the six cases. .... 67

**Table 21.** Numerical results for comparison of cases A and B. .... 68

**NOMENCLATURE**

$\dot{Q}$	Heat Duty, [W]
$\dot{W}$	Work, [W]
$\dot{m}$	Mass Flow Rate, [kg/s]
GL	Gas Loading, [-]
MF	Mass Fraction, [-]
MW	Molecular Weight, [kg/kmol]
R	Universal Gas Constant, [kJ/(kmol K)]
Z	Compressibility Factor, [-]
$e$	Specific Exergy, [kJ/kg]
$h$	Specific enthalpy, [kJ/kg]
$s$	Specific Entropy, [kJ/(kg K)]
$w$	Specific Work, [kJ/kg]

**Greek letters**

$\eta$	Efficiency, [-]
$\rho$	Density, [kg/m <sup>3</sup> ]

**Abbreviations**

AMR	Advanced Mixed Refrigerant
BOG	Boil-Off Gas
C3MR	Propane Pre-cooled Mixed Refrigerant
FLNG	Floating Liquefied Natural Gas
GHV	Gross Heating Value
GSU	Gas Sweetening Unit
HHC	Heavy Hydrocarbon
LNG	Liquefied Natural Gas
LPG	Liquid Petroleum Gas
NGL	Natural Gas Liquids
RVP	Reid Vapor Pressure
SMR	Single Mixed refrigerant
TPA	Tonnes Per Annum



# 1 INTRODUCTION

## 1.1 Background

In the coming decades, natural gas is expected to be the fastest-growing fuel source due to its abundance as a clean alternative to traditional fossil fuels. In the global market, Liquefied Natural Gas (LNG) provides a flexible way to transport the fuel, as well as a more economic method to export it across oceans, where pipelines have the disadvantages of operational difficulties and higher costs. The gas production in Australia and USA demands the creation of new LNG terminals to export the product, as European and Asian demand makes it necessary for new projects to adapt to this situation.

In the early phases of LNG projects, the profitability is usually based on the previous projects profitability or on simulations. Each project has numerous variables that make it unique, and therefore the estimations based on previous projects can lead to large deviations. On the other hand, the simulation tools need a high level of complexity and definition in order to perform accurate estimations. These simulations require a competent professional to interpret the results and understand the potential of the project and its feasibility.

The objective of this thesis is to develop a simplified model in order to estimate the production rates of different products obtained in a LNG plant, as well as the energy needs and the CO<sub>2</sub> emissions. The model will be designed to be implemented in Microsoft Excel, and it has to provide estimations within a relative error of +/-30% with respect to the real data. It must be able to cover a realistic range of configurations and conditions for the LNG plant, such as changing the compressor driver, the liquefaction process type and the feed gas arrival conditions.

## 1.2 Report structure

Chapter 2 presents the process description and the different product specifications. Chapter 3 presents the core of the thesis work on the modelling basis and block development, describing the model, the assumptions and simplifications, and developing each one of the subsystem models defined. Chapter 4 presents the model testing and the discussion of the results. Chapter 5 and 6 present the conclusion and the recommendation for future work.



## 2 PROCESS DESCRIPTION

The present chapter introduces the typical LNG plant layout, describing the different processes performed, as well as the power generation and location impact on the process. Besides, the different products are exposed together with their respective specifications

### 2.1 LNG production plants

The main process stages for typical LNG production plant are shown in Figure 1. The LNG production process and equipment will depend on the site conditions, feed gas conditions and composition, and on the final products specifications. Therefore, different LNG plants will have different configurations.

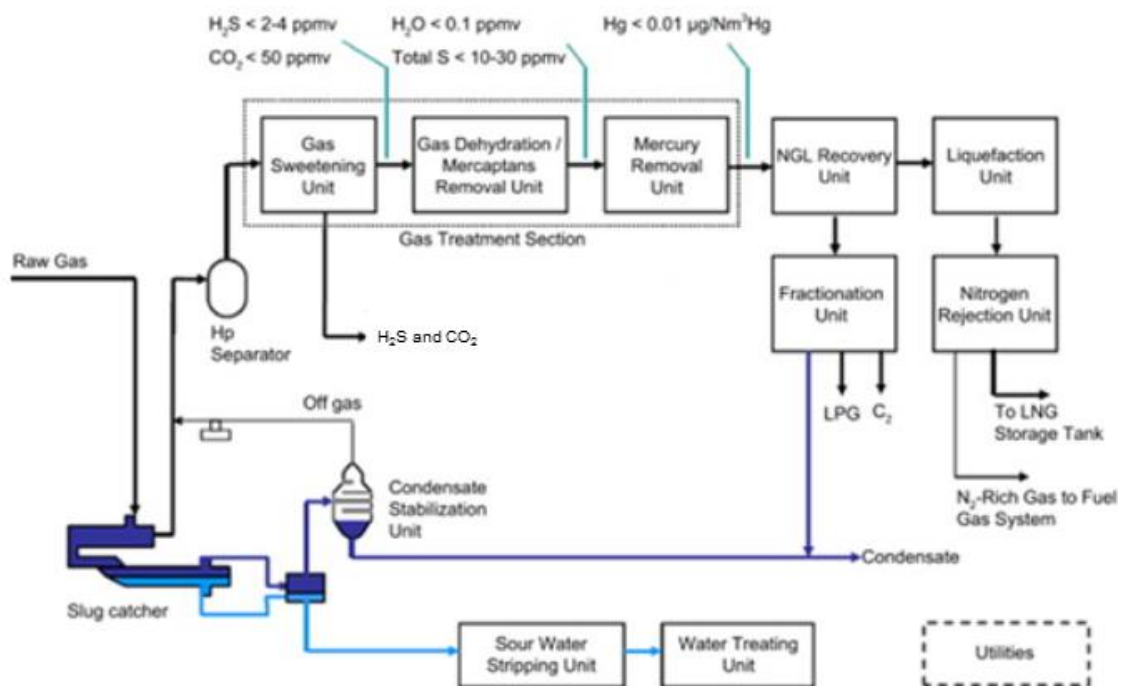


**Figure 1.** Typical LNG plant flow diagram (adapted from [1]).

Raw gas arriving from the wells is received and separated in a slug catcher. Gas is sent to the Gas Treatment Section, Hydrocarbon Liquids are sent to a Condensate Stabilization Unit, and liquid water is separated together with any hydrate inhibitor that has been injected in the transport system. The bottom condensate product consisting of C<sub>5+</sub> is stabilized to meet a Reid Vapor Pressure (RVP) specification.

Feed gas then enters the Gas Sweetening Unit (GSU), where CO<sub>2</sub> and H<sub>2</sub>S are removed. H<sub>2</sub>S is removed to meet the sales specification of 4 ppm of sulfur, whereas CO<sub>2</sub> must be removed to 50 ppmv to avoid freezing of this component inside the main heat exchanger of the liquefaction unit. To fulfill these strict requirements, amine-based processes are usually chosen to remove the acid gases.

Sweet gas obtained from the GSU enters a Dehydration Unit to remove the water by adsorption in molecular sieves. The gas coming out of the GSU is saturated with water that must be removed in order to avoid hydrate formation and freezing during the natural gas liquefaction. After dehydration, it is necessary to remove the mercury also by adsorption to avoid corrosion in the cryogenic heat exchanger, that takes place due to the reaction between the mercury and the aluminum in the cryogenic exchanger.

Dry gas is further sent to the NGL Extraction Unit, where C<sub>3+</sub> hydrocarbons are removed. This extraction can be either upstream or integrated in the liquefaction process. The NGL extraction is necessary to fulfill the Gross Heating Value (GHV) specification, as well as to reduce the risk of freezing of heavy hydrocarbons during the liquefaction process. Besides, LPG components are valuable market products which are separated from the rest to obtain pure components and make-up refrigerant.

The gas obtained after the processing is then liquefied. The liquefaction and subcooling process of gas is based on a refrigeration cycle which takes place at gliding temperature and close to constant pressure.

After the liquefaction it is necessary to remove any excess nitrogen to meet the sales specifications below 1 mol% of nitrogen. The pressure of the LNG is decreased to a few bars due to storage and transport requirements inside the End flash section of the plant, and during this expansion the nitrogen, being a lighter component, is flashed off together with methane from the LNG. This End flash gas, together with the Boil-off gas (BOG) from the storage tanks, is generally used as fuel gas for the gas turbines driving and/or supplying power to the LNG plant.

The large needs of power for LNG production is usually covered by gas turbines. These gas turbines can be either industrial or aeroderivatives, with the first one as the most common choice. Besides, nowadays the option of importing energy from the electrical grid is an option.



Several projects are considering the use of this last option to partly or fully cover the driver and power needs of the LNG plant.

## **2.2 Location impact on the process**

The climate has a large effect in the energy consumption and production, as well as in the production capacity of the plant. The ambient air temperature directly affects the power output of the gas turbine, as the warmer the air is the lower this output will be. This leads to an increase in the fuel gas consumption to keep the same level of power production, and therefore to the decrease of the production capacity. Besides, it affects the refrigeration system efficiency of the plant, as the heat rejection temperature of the refrigerant will depend also on the climate. The lower the cooling system is able to cool the gas before entering the liquefaction process, the less energy it will require,

## **2.3 Product specifications and requirements**

### **2.3.1 LNG plant products**

The different products obtained from the LNG plant have different specifications depending on the final product requirements. LNG product specifications are very strict in order to fulfil the sales requirements. Typical specifications provided by [2] are listed in the following sections.

Sales products are the Condensate, the LPG and the LNG. The Natural Gas Liquids (NGL) are fractionated in order to obtain make-up refrigerant, whereas the LNG is the main product obtained from the process.

There are other “products” obtained from the plant: fuel gas, carbon dioxide and nitrogen. The fuel gas is necessary to drive the gas turbines of the process and to produce power, and it can be taken from the feed gas stream, the End flash gas, the Boil-off gas from the storage tanks and the vapor return from the ship. The CO<sub>2</sub> is obtained from the feed gas and from the gas turbines combustion. This CO<sub>2</sub> is usually vented to the atmosphere, but due to more restrictive laws about the climate change, CO<sub>2</sub> storage is increasing its importance in LNG plants. Finally, the nitrogen is removed from the gas stream through the End flash to fulfill the LNG product requirements.

### 2.3.2 LNG specifications

The LNG product must fulfill the specifications defined in Table 1, which are based on composition mol%. Besides, it is necessary to mention that the LNG product must be stored at atmospheric pressure.

**Table 1.** LNG component specifications.

Component	Unit	Minimum	Maximum
Nitrogen	mol %	-	1.00
Methane	mol %	85	100
Butane	mol%	-	2.00
C <sub>5+</sub>	mol%	-	0.1
CO <sub>2</sub>	ppmv	-	50
H <sub>2</sub> S	ppmv	-	4

#### Quality aspects

There is one LNG quality parameter that has been taken into account during this thesis: the Gross Heating Value (GHV).

The GHV can be defined as the amount of heat that is released during the combustion of a substance including the condensation of water from the combustion. As the gas usually consists of a mixture, it is necessary to perform different calculations in order to obtain a value of the GHV for a specific composition. Further information about the calculations can be found in Section 3.4.6.

The desired GHV depends on the end user of the product, and its value has to be modified by varying the LNG composition. Figure 2 presents examples of GHV ranges depending on the region.

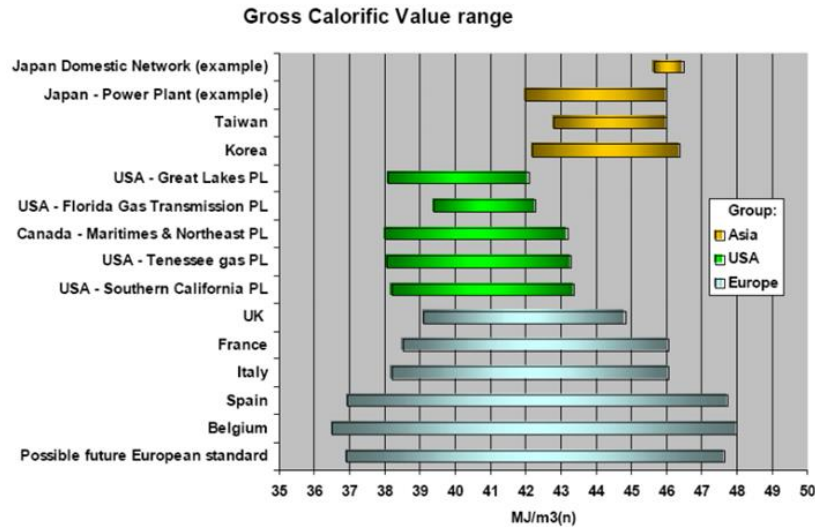


**Figure 2.** Examples of Gross Calorific Value ranges [3].

### 2.3.3 Condensate specifications

There is one condensate specification that has been used in the present thesis; the RVP, specified in Table 2. Other specifications have not been taken into account in the present work.

**Table 2.** Condensate specifications.

Parameter	Specification
Reid Vapour Pressure (RVP)	<11.5 psia at 37.8 °C

### 2.3.4 LPG specifications

For the LPG, there are two main component specifications stated in Table 3 that this product has to fulfill.

**Table 3.** LPG component specifications.

Component	Unit	Minimum	Maximum
Ethane	% mol	-	1.00
C <sub>5+</sub>	% mol	-	2.00



### 3 MODELLING BASIS AND DEVELOPMENT

#### 3.1 Modelling Software

The model design has been based on two different software in order to obtain the required expressions. Aspen HYSYS has been used to analyze the behavior of the different processes and obtain simple expressions representing them, whereas Microsoft Excel has been used as a platform where all the expressions have been implemented to test the model validity.

##### 3.1.1 Microsoft Excel

The proposed model has been implemented in Microsoft Excel, and the complexity level of the model has been defined consequently to allow its implementation in this spreadsheet software. To accomplish it, each subsystem model has been defined as independent from the others as possible, avoiding interdependencies between the different subsystem models that led to a high level of complexity. Besides, different assumptions and simplifications have been formulated to facilitate the definition of the model.

##### 3.1.2 Aspen HYSYS

Aspen HYSYS is a process simulation tool that has been used to obtain and validate the mathematical models defined. The different processes in a LNG plant contain several parameters that cannot always be approximated by simple equations. Through HYSYS, some of these models have been studied to obtain an insight of the process and evaluate the impact of the different parameters' variation on the energy and mass balance, as well as the CO<sub>2</sub> emissions. These evaluations have permitted to state different assumptions that cause the smallest possible deviation within the different simplification opportunities.

When possible, in-built models from HYSYS have been used to avoid spending excessive time modelling the processes. In case no in-built models were suitable for the task to be performed, simplified models have been set to a given reference data, and then their behavior studied to obtain an expression appropriate for the spreadsheet model.

### 3.2 Objective parameters

The present project has been created to estimate the mass and energy balance, as well as the CO<sub>2</sub> emissions. Table 4 includes the six different streams from the process that are split into sales products and additional products. Further discussion about the different streams is discussed in Section 3.3.1.

**Table 4.** Main products obtained from the process.

Sale product	Additional products
LNG	Fuel gas
LPG	Carbon Dioxide
Condensate	Nitrogen

The energy balance has been split in heat and work duties. Each subsystem model provides estimations of the energy consumption that serves to obtain an approximation of the energy needs in the entire plant. Figure 3 presents the basis for the proposed model. Feed gas is split in three different sales products, fuel gas, nitrogen and CO<sub>2</sub> through the addition of electrical power and heat.

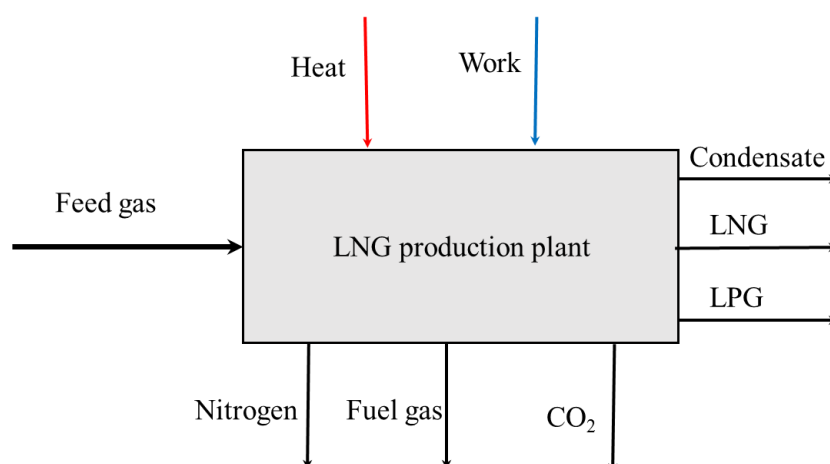


**Figure 3.** Simplified block diagram of the proposed model.

### 3.3 Basis for LNG plant model

Figure 4 represents the procedure that was followed during the present thesis to achieve the objective parameters. The behavior of the different processes was defined from literature research, real plant data and process simulation. This behavior was studied and simple equations were defined from them, so the model could be implemented in a spreadsheet software. Finally,

the objective parameters were calculated from different input parameters, and these results were benchmarked against real data.

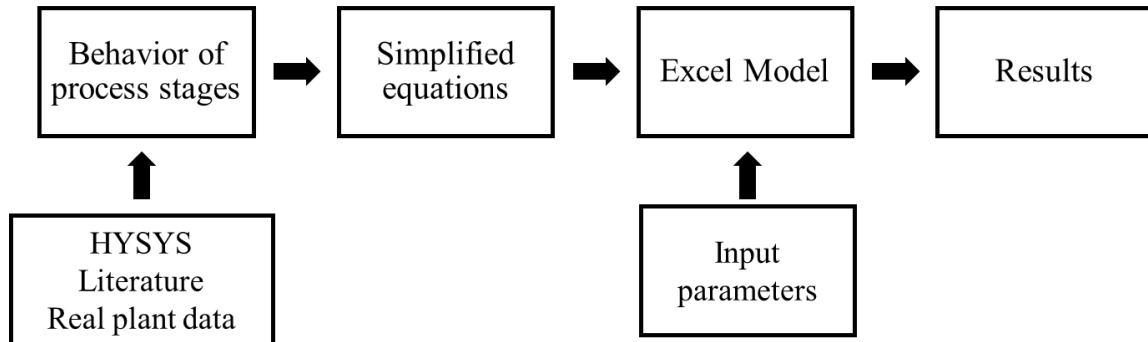


**Figure 4.** Process to create the model.

### 3.3.1 User inputs

The model has been designed as flexible as possible to include the largest amount of LNG plant configurations. However, it has been necessary to limit the possible situations in order to obtain reliable results without involving too much complexity. To perform the estimations, the user has to define different parameters that have been restricted in different manners.

Table 5 presents the different parameters that are defined by the feed gas as the ambient, as well as the desired number of yearly operation days so the yearly production of the different products can be estimated.

**Table 5.** Definition of the feed gas parameters, ambient parameters, and number of yearly operation days.

	Parameter	Units
<b>Feed gas parameter</b>	Flow rate	ton/h*
	Composition (C <sub>1</sub> to C <sub>5</sub> , C <sub>6+</sub> , N <sub>2</sub> and CO <sub>2</sub> )	mol%
	Arrival pressure	bar
<b>Ambient parameters</b>	Mean air temperature	°C
	Mean water temperature	°C
<b>Number of yearly operation days</b>		days

\*if desired, the flow rate can be provided in MSM<sup>3</sup>/day, and the model will calculate the ton/h

Table 6 presents the different technical options that the model require to perform the different estimations. In order to estimate the objective parameters it is necessary to define the liquefaction process type (see Section 3.4.5 for further information), the cooling method and the driver.

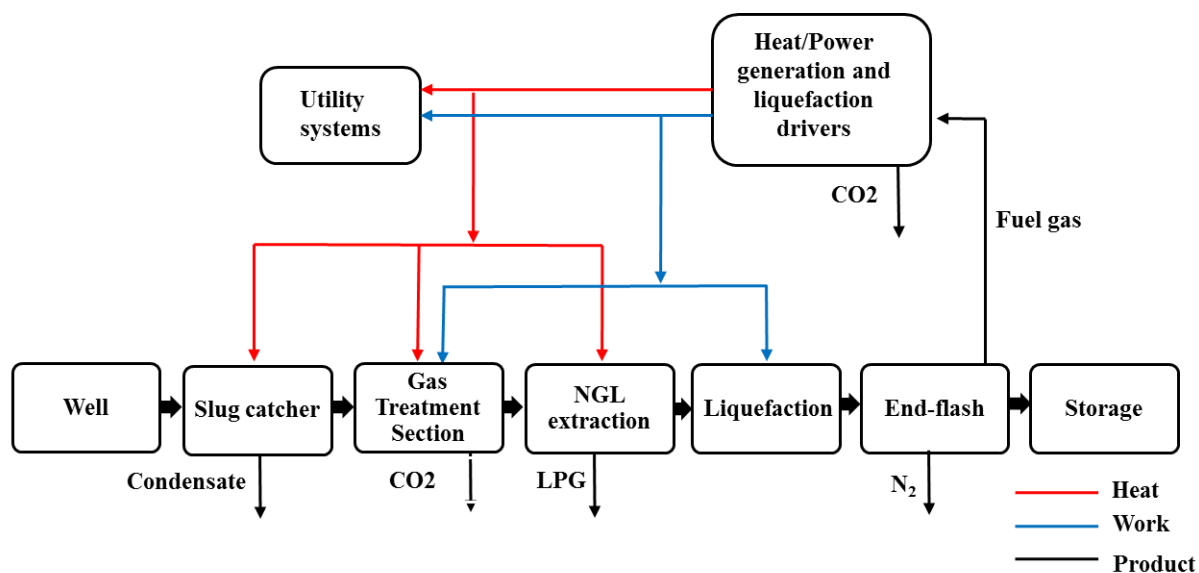
**Table 6.** Plant parameters that require a technical decision for the plant estimations.

Plant parameter	Options
Liquefaction process type*	AMR/C3MR
	SMR
	N <sub>2</sub> expander
Cooling method	Water
	Air
Driver	Industrial Turbine
	Aeroderivative Turbine
	Electrical grid
LNG product richness	Lean
	Medium
	Rich
LPG production	Yes/No

\*Advanced Mixed Refrigerant (AMR) includes Dual Mixed Refrigerant and Mixed Fluid Cascade. C3MR stands for Propane Precooled Mixed Refrigerant, and SMR for Single Mixed Refrigerant

### 3.3.2 Model layout

Figure 5 presents the model layout of the entire plant. The plant has been split in different process blocks. This section explains the main features of the model defined, whereas more detailed explanations about the calculation basis, assumptions and simplifications of each block are discussed in Section 3.4.

**Figure 5.** Principle sketch for the proposed model.

Feed gas at given temperature, pressure and composition enters the separation model which includes the slug catcher and the Condensate stabilization. This model removes all the C<sub>5+</sub> content of the feed gas.



Light gas enters the Gas Treatment Section, which is divided in two subprocesses. The Gas Sweetening Unit model, which removes all the CO<sub>2</sub> contained in the feed gas, and the Dehydration Unit model, which takes away all the water from the gas stream. These processes need heat and electrical power. The CO<sub>2</sub> removed is taken into account for the final CO<sub>2</sub> emissions estimation, whereas the water flow rate is not further taken into account.

The model has not accounted for the Mercury Removal Unit, and therefore dry gas enters the NGL Extraction model. The heat duty of this model is calculated for the de-ethanizer reboiler, and a split ratio has been defined for the different options available.

Gas leaving the NGL Extraction model enters the liquefaction model, where work is added to drive the process. Later, the liquefied gas is expanded and separated in the End flash. A split ratio for the nitrogen has been defined to fulfill the final LNG product specification and the GHV of the fuel gas that is always assumed to be taken from the End flash (See Section 4.3.5).

Besides the main process, a utility system block corrects the energy calculations to account for the subsystems that were not modelled.

The heat and electrical power needs are assumed to be covered by the driver choice. If the choice is a gas turbine, fuel gas is consumed to drive the liquefaction process and to produce electrical power, whereas the waste heat produced covers the heating needs. In case the electrical grid is chosen, the grid covers the liquefaction compressors and the electrical power needs whereas fuel gas is consumed to cover the heating needs.

## **3.4 Block development**

### **3.4.1 Process temperature definition**

Air and water cooling systems are used in the present model to set the minimum process temperature in the plant. It has not been addressed the possibility of hybrid cooling systems.

The air and water temperatures have been based on yearly mean temperatures, and then no yearly variations have been accounted in the model. For the case of the water cooling system, it has not been differentiated between direct or indirect cooling. The effect of the minimum temperature approach between the heat sink and the process stream has been analyzed. Different approach temperatures were used in the model and compared against the reference cases [2],

and it was decided to set the approach temperature to 15 °C for the air cooling system and to 10 °C for the water cooling system as they provided the highest accuracy.

### 3.4.2 Separation

It has not been possible to obtain a heat duty estimation for the condensate stabilization due to the inaccuracies in the model approach (See Appendix A). Instead, the heat needs of this unit are taken into account in Section 3.4.7 through the heat duty scaling factor. Two products are obtained from it: the light gas that is sent to the Gas Treatment Section, and the Condensate that is stored. For simplicity, all the C<sub>5</sub> and C<sub>6+</sub> are assumed to be removed in this model, implying that no C<sub>5+</sub> is later removed in the NGL extraction model. As the HHC are defined as C<sub>6+</sub>, the molecular weight of the hexane has been used to represent the C<sub>6+</sub> molecular weight. The water and MEG removal has not been included. Therefore, the feed gas has been assumed free of them.

### 3.4.3 Gas Treatment Section

The Gas Treatment Section model is divided in two subsystem models: Gas Sweetening Unit for the CO<sub>2</sub> removal and Dehydration Unit for the water removal.

#### Gas Sweetening Unit

This model consists on a MDEA absorption unit. It has two products: CO<sub>2</sub> as final product, and the sweetened gas. The H<sub>2</sub>S has not been accounted as a different stream due to the assumed negligible traces in the gas. The model takes into account the heat duty for the MDEA regenerator, as well as the electrical power consumed by the solution pump.

The GSU is an important unit of the overall model for two reasons: it can highly contribute to the CO<sub>2</sub> emissions in case the feed gas contains large amounts of it, and it is one of the main heat consumers of the LNG plant. Thus, focus has been destined to this unit. This model has not accounted for the possibility of storing the CO<sub>2</sub>, and therefore it is all taken into account for the overall CO<sub>2</sub> emissions of the plant.

The largest amount of heat duty is used to strip away the CO<sub>2</sub> and produce lean amine in the regenerator to reuse it again in the absorber. This energy can be calculated from the mass flow rate of amine [4]. The amine mass flow rate is defined by Equation [3.1] as follows:

$$\dot{m}_{amine} \left[ \frac{kg}{hour} \right] = \frac{(\dot{m}_{feedgas})(MF)(MW)}{(GL)} \quad [3.1]$$

Where:

- $\dot{m}_{amine}$  [kg/hour] is the circulation flow rate of the amine
- $\dot{m}_{feedgas}$  [kmol/hour] is the feed gas flow rate
- $MF$  [(mol CO<sub>2</sub>/mol feed gas)] is the total CO<sub>2</sub> mol% in the feed gas
- $GL$  [(mol acid gas)/(mol amine)] is the acid gas loading
- $MW$  [kg/mol] is the molecular weight of the amine (119.2 for MDEA)

To provide an effective acid gas removal within an acceptable level of corrosion, a solution loading of 0.5 [mol acid gas/mol gas] and a strength of 50% [kg amine/kg solution] have been used. Besides, the amine final flow rate has been increased by 20% to provide excess amine and ensure a correct performance of the unit. These decisions, together with the decision of using MDEA, makes possible to calculate the mass flow rate of amine as a function of the total CO<sub>2</sub> content in the feed gas through Equation [3.2].

$$\dot{m}_{amine} \left[ \frac{kg}{hour} \right] = 6.5 \dot{m}_{CO_2} \quad [3.2]$$

Where  $\dot{m}_{CO_2}$  [kg/h] is the CO<sub>2</sub> mass content in the feed gas.

The reboiler duty has been obtained based on the GPSA data book [5] which provides approximated guidelines for amine processes. In agreement with these guidelines, the reboiler duty has been expressed for a specific duty between 220-250 kJ/kg of lean solution. Equation [3.3] defines the reboiler duty, and this duty has been set for the higher recommended value in the reference to provide a conservative heat duty value. For simplification, the already calculated rich solution has been used instead of the lean one stated in the reference.

$$\dot{Q}_{GSU} [kW] = 0.066 \frac{\dot{m}_{amine}}{WF} = 0.86 \dot{m}_{CO_2} \quad [3.3]$$

Where:

- $\dot{Q}_{GSU}$  [kW] is the heat duty in the reboiler
- WF [(kg amine)/kg solution] is the amine weight fraction
- $\dot{m}_{amine}/WF = \dot{m}_{solution}$  [kg/h] is the mass flow rate of the total amine solution

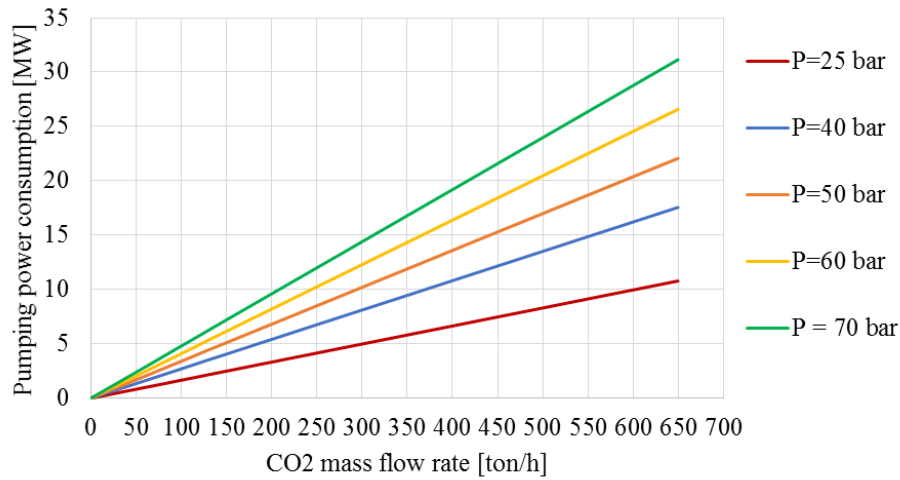
To obtain the solution pump power it has been necessary to use an MDEA model available in Aspen HYSYS V8.6. The expression of the solution pump power has been modelled to account for the variation of acid gas content and the variation of the feed gas arrival pressure (See Appendix B). Once the relationship between the CO<sub>2</sub> and the amine flow rates has been defined by Equation [3.2], it is possible to express the solution pump power with respect to the CO<sub>2</sub> contained in the feed gas. The inlet temperature of the feed gas has been maintained to 30 °C during the calculation of the expression. Due to the linearity of the function, it was firstly approximated a linear expression to define it. However, the order of magnitude of the linear expression was of 10<sup>-4</sup>. For this model, such low orders of magnitude were avoided, and for that reason, it was decided to use a logarithmic approximation which, after testing it, provided results with the same accuracy as the linear one within the defined range of use.

$$\dot{W}_{Amine\ pump} [kW] = 6.5e^{1.02 \ln(P) - 9.25} * \dot{m}_{CO_2} \quad [3.4]$$

Where:

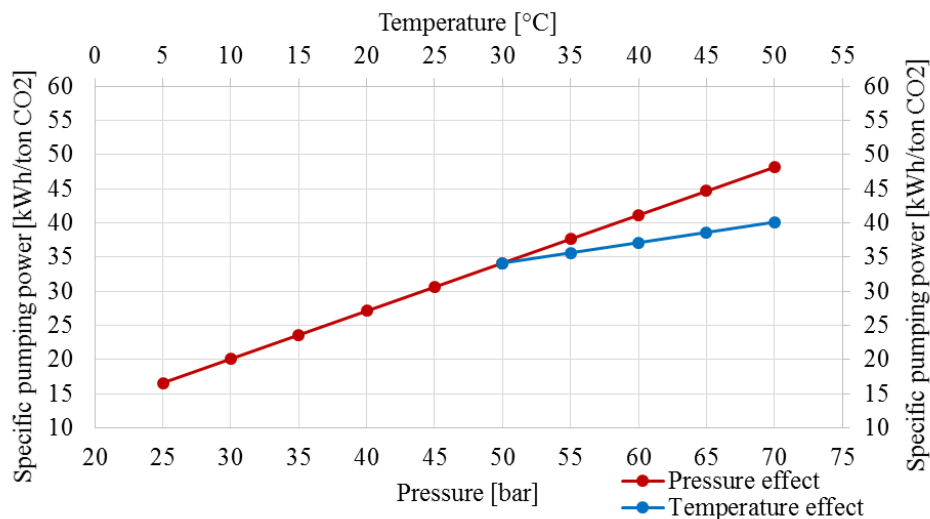
- $\dot{W}_{Amine\ pump}$  [kW] is the solution pump power
- P [bar] is the feed gas pressure

Figure 6 presents the variation of the solution pump power for different pressures depending on the mass content of CO<sub>2</sub> in the feed gas.



**Figure 6.** Solution pump power for different pressures as a function of the total CO<sub>2</sub> mass flow rate.

It was acknowledged that the feed gas inlet temperature affects the power. However, it has been necessary to neglect its contribution for simplification. Its relative effect to the power consumption is minor when compared to the pressure effect. The specific power by ton of CO<sub>2</sub> absorbed as a function of the pressure and temperature has been presented in Figure 7 for a CO<sub>2</sub> 4 mol%. Both the temperature and pressure are presented within the possible operational range of this unit. The range of temperature has been set according to the limitations of the amine, as a minimum temperature of 30 °C is necessary for the reaction, but temperatures higher than 50 °C can lead to thermal degradation of the amine.



**Figure 7.** Specific pumping power variation depending on the feed gas pressure and temperature for a CO<sub>2</sub> content in the feed gas of 4 mol %.

The addition of a preheater was studied to account for the temperature effect, but due to unknown temperature after the condensate stabilizer, and the low relative effect it had within the entire model, it was decided to not add it so the complexity level was not increased.

### Gas Dehydration Unit

The dehydration model has one product: dry gas that is sent to the NGL extraction. The water removed is taken away from the process. The dehydration contribution to the energy balance consists on the heat needed for the regeneration process of the molecular sieves.

After the CO<sub>2</sub> is absorbed, the gas is washed with water to remove the amine traces. Due to this, the sweetened gas is saturated with water that has to be removed by adsorption in molecular sieves. These sieves must be regenerated by heat addition.

Different approaches were considered. Firstly, a model was simulated in HYSYS basing the process on a simple splitter. For a defined split ratio, the simulation calculated the heat duty needed to carry out the separation. The results obtained from the model were compared to reference data [2] and there was a relative error of +66% with respect to the reference heat duty, what invalidated the model in HYSYS. Alternatively, it was decided to use an analysis of the adsorption process performed by PetroSkills [6] in order to obtain an expression for the heat duty as a function of the gas flow rate.

The water content in the gas is highly affected by the temperature, pressure and flow rate of the gas, and consequently different correction factors have been considered for each one of the parameters. The reference state has been set to 30 °C and 50 bar, and the factors have been expressed as the variation in heat duty with respect to the reference conditions. Further explanation of the simplifications and definition of the expressions can be found in Appendix C.

An expression has been obtained from [6] to approximate the heat duty depending on the gas flow rate. Equation [3.5] represents this heat duty variation at reference conditions, where  $\dot{m}_{gas}$  [ton/h] represents the total flow rate of the gas at the dehydration model inlet.

$$\dot{Q}_{Dehydration,ref}[MW] = (0.03\dot{m}_{gas} - 0.7) \quad [3.5]$$

Figure 8 represents this variation of the heat duty depending on the gas mass flow rate. It has been assumed valid for flow rates larger than the range defined for the definition of the expression.

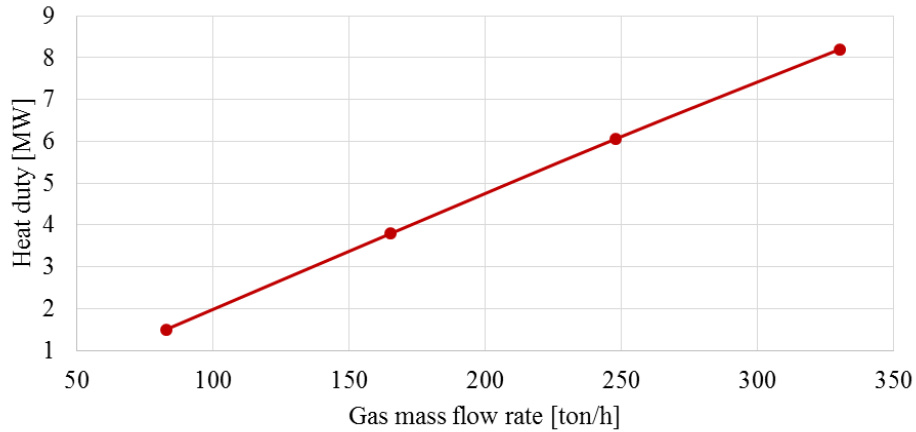


**Figure 8.** Dehydration heat duty as a function of the total gas mass flow rate.

The pressure to be provided in the model is the arrival pressure, and for the temperature, because it has not been assessed an evaluation of the gas temperature after the GSU, it has been decided to use the minimum process temperature achieved after cooling the gas stream.

The pressure correction factor has been defined by Equation [3.6], where the pressure is defined in absolute bar.

$$F_p = -0.007P + 1.37 \quad [3.6]$$

The temperature correction factor has been defined by Equation [3.7] where the temperature is defined in °C.

$$F_T = 0.06T - 0.76 \quad [3.7]$$

Figure 9 presents the percent variation of the heat duty defined by the two correction factors defined before.

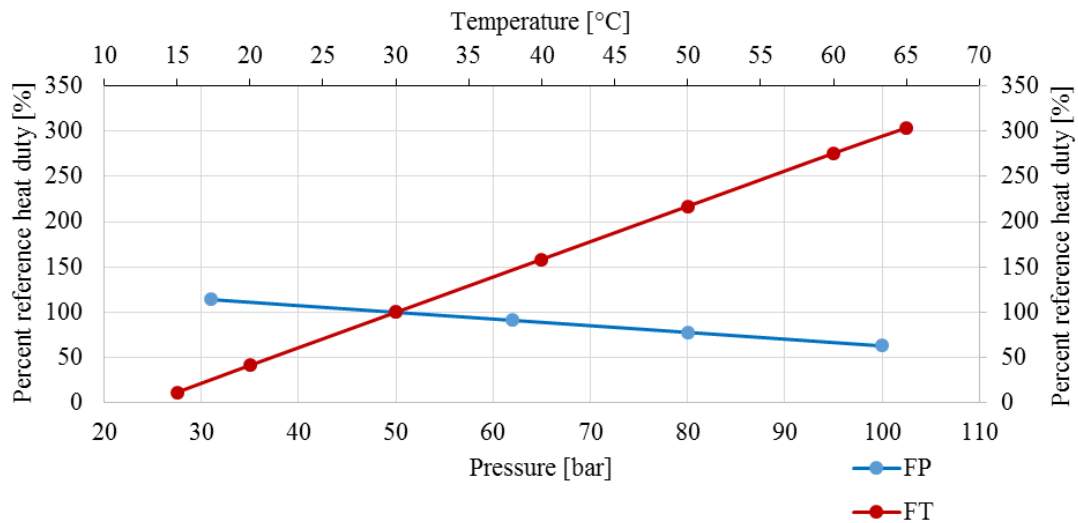


**Figure 9.** Graph representing the effect of the pressure and temperature on the heat duty. Each line represents the percentage variation of the head consumption depending on each parameter.

Once the factors have been obtained, it is possible to find the regeneration heat duty for the dehydration process from Equation [3.8]. The accuracy of this expression is limited to a lowest process temperature of 15 °C. Below this value, the model does not provide reasonable values of the heat duty.

$$\dot{Q}_{Dehydration}[MW] = (0.03\dot{m}_{gas} - 0.7) * F_P * F_T \quad [3.8]$$

### 3.4.4 NGL Extraction

This subsystem model provides two different products: gas that is sent to the liquefaction unit, and LPG as final product. This model only accounts for upstream extraction, and it accounts for heat duty necessary to separate the ethane from the LPG, assuming the methane has been previously separated in a scrub column.

To model this unit, it has been necessary to define whether there is LPG production or not in order to calculate the LNG mass flow rate consequently. Besides, it has been necessary to define the richness level of the LNG product such that is possible to delimit its C<sub>3</sub> and C<sub>4</sub> content in case LPG is also produced.

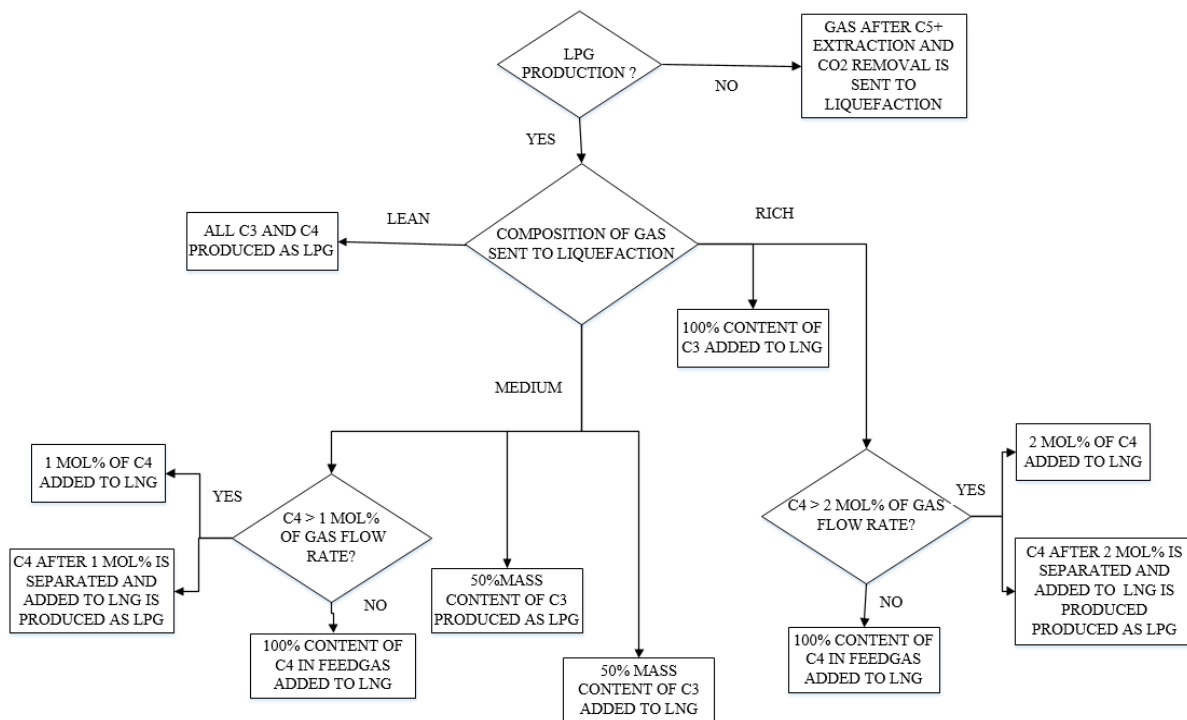
The composition options have been divided in three ranges depending on the methane content in order to address the LNG richness: lean, medium or rich gas. Table 7 presents the defined ranges for each composition classification depending on the methane mol%.



**Table 7.** Definition of the composition range of the liquefied gas components depending on the methane mol%.

Composition	C <sub>1</sub> Minimum [mol%]	C <sub>1</sub> Maximum [mol%]
Lean	93.6	100
Medium	87.6	93.5
Rich	85	87.5

Figure 10 presents the flow diagram of the algorithm modelled to calculate the mass balance in the unit. Firstly, it is necessary to know whether LPG is produced or not. After this option is defined, the richness level of the LNG product is set. In case there is LPG production and it is also desired to obtain a medium or rich LNG product, the richness level defines the split ratio between the LPG and the LNG product. If there is not LPG production, the richness level is taken into account in Section 3.4.5 due to its effect on the power needs to drive the compressors in the liquefaction process.

**Figure 10.** Flow diagram for the mass balance calculation in the NGL extraction unit.

In case LPG is produced, the lean classification assumes that the gas entering the liquefaction only contain C<sub>1</sub>, C<sub>2</sub> and nitrogen. The reason of not taking into account the C<sub>3+</sub> is to differentiate better between the lean and de medium classification. For the medium and rich cases, the C<sub>3</sub> mass fraction is based on the total C<sub>3</sub> content in the feed gas, whereas the C<sub>4</sub> mol% is calculated based on the gas composition at the inlet of the NGL extraction unit. Once the composition of the gas sent to liquefaction is defined, the excess of C<sub>3</sub> and C<sub>4</sub> is produced as LPG.

Table 8 indicates how the LPG entering the liquefaction model is distributed for the medium and rich classifications. The split ratio was based on the reference data [2], where only one case had LPG production.

**Table 8.** Definition of the gas entering the liquefaction unit for each richness classification. These split ratios are only applied when LPG is produced.

Component	Medium	Rich
C <sub>3</sub>	50% mass content in feed gas	100% mass content in feed gas
C <sub>4</sub>	1 mol%	2 mol%

A HYSYS simulation was modelled to obtain the heat duty of the de-ethanizer reboiler. A column with a reboiler and a condenser was used for this task. Due to the operational performance of the column, it was necessary to set the pressures inside the column as well as the feed gas inlet parameters. Besides, the different specifications were evaluated. Two different specifications were used for the model definition: overhead C<sub>2</sub> mol fraction of 94 %, and C<sub>2</sub>/C<sub>3</sub> bottom ratio of 0.02.

This model has been analyzed for feed gas temperature and pressure variation, as well as the composition. For a defined composition, the feed gas pressure and temperature were varied to study their effect on the heat duty. Reference feed gas parameters were set to 30 °C and 50 bar. Then, the temperature was varied between 10 and 65 °C, and the pressure between 25 and 100 bar. Figure 11 presents the effect these parameters have on the de-ethanizer reboiler duty with respect to the reference conditions.

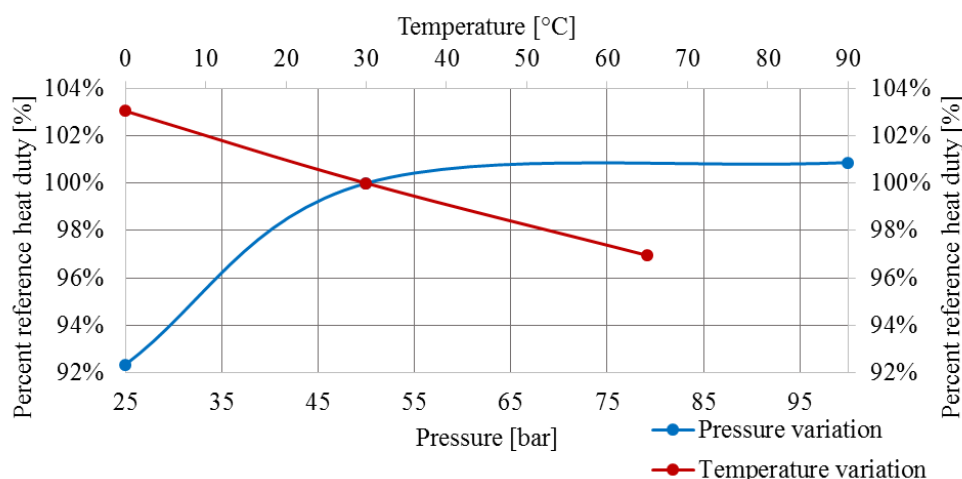


**Figure 11.** Heat duty variation of the de-ethanizer reboiler depending on the feed gas temperature and pressure.

After this analysis, it was decided to neglect the effect these parameters had because it would have meant an increase in the complexity of the expression. Instead, it was decided to account for the composition variation, due to its larger effect.

The composition effect has been studied under different simplifications due to the difficulties of defining a general expression for all kinds of compositions. It has been assumed that all the methane has been previously removed. Therefore, the gas flow rate contains all the C<sub>2</sub>, C<sub>3</sub> and C<sub>4</sub>. Figure 12 represents the specific reboiler duty per kg of gas entering the de-ethanizer for different compositions. C<sub>2</sub> has been increased from 40 to 70 mol%, and for each C<sub>2</sub> mol fraction the C<sub>3</sub> has been varied. The remaining part of the gas is considered C<sub>4</sub>.

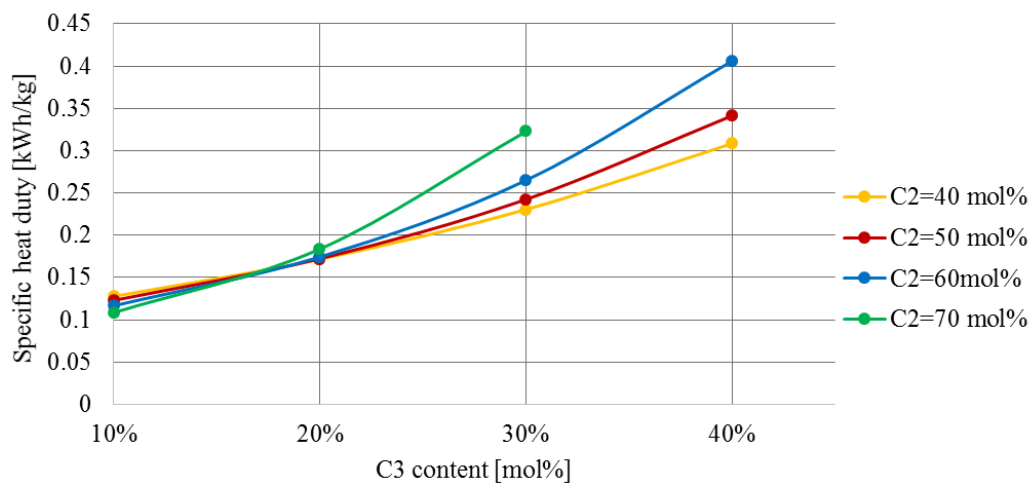


**Figure 12.** Specific heat duty of the de-ethanizer reboiler depending on the composition.

As it is observed from the figure above, the LPG composition affects the heat duty. For this reason, it has been necessary to obtain an expression of the heat duty as a function of the mol fraction of C<sub>2</sub> and C<sub>3</sub>. To simplify, the composition is based on the NGL Extraction Unit inlet composition, assuming all the C<sub>1</sub> and N<sub>2</sub> are removed upstream the de-ethanizer. It is assumed that all the C<sub>2+</sub> enters the de-ethanizer, and then it is later fractionated and/or reinjected to the main gas stream that enters the liquefaction unit.

It has been assumed that the entire amount of C<sub>2</sub> is always liquefied and produced as LNG, regardless the definition of the LNG product richness. This simplification has been done to avoid further complications with the split ratio in the NGL Extraction model.

The necessity of accounting for both components has increased the complexity level of the model, but it had to be done to estimate this unit in order to get more information about the heat

needs of the LNG plant and reduce the final scaling factor that infers large uncertainties. This variation of the composition has been approximated by the exponential expression [3.9] (see Appendix D).

$$\dot{Q}_{de-ethanizer}[MW] = \dot{m}_{de-ethanizer}(-0.11[C_2] + 0.14)e^{(20.6[C_2]-14.3[C_2]+5.4)*[C_3]} \quad [3.9]$$

Where:

- $\dot{m}_{de-ethanizer}$  [kg/h] refers to the total C<sub>2+</sub> at the inlet of the NGL extraction unit
- $[C_2]$  is the mol fraction of ethane
- $[C_3]$  the mol fraction of propane

Equation [3.9] has to be used within the composition range analyzed. Very low ethane content relative to the propane mol% leads to a high specific power per kg of mass flow rate, and for these situations, the de-ethanizer should be modelled differently to correctly estimate its duty.

### 3.4.5 Liquefaction unit

This unit is based on exergy calculations, and its only product is LNG at 1.1 bar. Therefore, the calculations do not only account for the liquefier, but the End flash to fulfill the specifications. However, the End flash gas calculations are further assessed in Section 3.4.6. The power consumption of this unit is all addressed to the compressor power requirement of the liquefaction unit.

As stated in previous sections, the model accounts for four different liquefaction process types: Advanced Mixed Refrigerant (AMR), which includes Dual Mixed Refrigerant (DMR) and Mixed Fluid Cascade (MFC), Propane Pre-cooled Mixed Refrigerant (C3MR), Single Mixed Refrigerant (SMR) and N<sub>2</sub> expander process. Besides, three different correction factors have been obtained to address the feed gas temperature, pressure and feed composition effect on the power needs.

In first instance, HYSYS models were considered for each one of the process types. To correctly model these processes, it was necessary to optimize the refrigerant composition depending on the feed gas composition. The optimization of the mixed refrigerant composition implied a thorough procedure that resulted to be unreasonably complex for the present model.

Therefore, this option was rejected, and it was decided to use an exergy analysis that implied simple calculations and easiness to account for the different aspects of the process, obtaining a flexible expression valid for its implementation in Microsoft Excel.

The exergy difference between inlet and outlet of the process is used to estimate the total available work between the two states. This difference is calculated through the enthalpy and entropy of each state using Equation [3.10]. For that, the outlet state has been used as reference state, fixing the pressure of 1.1 bar and the bubble point temperature of the LNG (-161.7 °C for the reference pressure and composition). The inlet state has been varied to include the effect of the variation in temperature and pressure of the gas entering the unit in the model. The heat rejection temperature of the process (see Section 3.4.1) has been used to define the feed gas inlet temperature, whereas the pressure, affecting the enthalpy and entropy, has been set to the arrival pressure.

$$\Delta e_{1-2} \left[ \frac{kJ}{kg} \right] = (h - T_0 s)_{LNG} - (h - T_0 s)_{feed} \quad [3.10]$$

Where:

- $e$  [kJ/kg] is the specific exergy
- $h$  [kJ/kg] is the specific enthalpy
- $T_0$  [°C] is the heat rejection temperature of the process
- $s$  [kJ/kg] is the specific entropy

Once the total reversible work is calculated, it is necessary to account for the specific efficiency of the liquefaction process type, in order to estimate the power need of each specific process type.

### Efficiency calculation

The reference efficiency calculation has been based on reference specific power requirements for the different process types [2]. Equation [3.11] defines the calculation of the exergy efficiency, which compares the total reversible work during the liquefaction against the real power requirements of the process itself. These efficiencies are consistent with the use of the mass flow rate at the liquefaction inlet.

$$\eta_{exergy}[-] = \frac{\Delta e_{1-2}}{w_{real}} \quad [3.11]$$

Where  $w_{real}$  [kJ/kg] is the real work obtained from the reference data and  $\Delta e_{1-2}$  [kJ/kg] is the exergy difference at reference inlet and outlet state for the lean gas composition.

The exergy difference used for the efficiency calculation has been the obtained for the lean gas case stated in Table 10 because the reference data is referred to a lean gas. These efficiencies have been kept constant at all times, assuming they are not affected by the parameters considered in the correction factors. Table 9 presents the three different efficiencies that have been obtained for the characterization of the model. AMR and C3MR processes are assumed to have the same efficiency due to minor differences. The relative efficiency of these processes has been validated against additional reference data [7].

**Table 9.** Exergy efficiencies of the different process types.

Process type	Exergy efficiency [-]	Relative AMR/C3MR
AMR, C3MR	0.45	100
SMR	0.41	91
N <sub>2</sub>	0.32	71

### Correction factors

Three different factors have been necessary to reflect the inlet process temperature, feed pressure and composition variations. These factors are modelled to reflect the percent variation in reversible specific work with respect to the reference inlet state mentioned above.

Two independent correction factors have been obtained for the temperature and pressure correction. A correction factor for the composition effect was obtained following the same principle as the temperature and pressure factors to reflect the exergy difference variation as a result of the composition variation. For simplification, the temperature and the pressure factors are assumed to be valid regardless the gas composition variation, whereas the composition correction factor has been assumed to be valid for every temperature and pressure within the stated range.

The pressure correction factor has been obtained for a pressure range between 25 and 100 bar. This factor has been defined by Equation [3.12] where the pressure is expressed in absolute bar.

$$K_P[\% \text{ reference}] = -0.27 \ln(P) + 2.06 \quad [3.12]$$

The pressure effect has been tried with a polynomial and a logarithmic expression in order to choose the most accurate approximation. After the analysis, the logarithmic expression was chosen due to its better definition of the process energy needs within the defined range of study.

The temperature correction factor has been obtained for a temperature range between 0 and 65 °C. This factor has been expressed by Equation [3.13] where the temperature is expressed in °C.

$$K_T[\% \text{ reference}] = -0.01T + 0.74 \quad [3.13]$$

For  $K_T$ , a linear and a polynomial expression were tried. In this case, the linear expression better fit the temperature variation.

Further information about the approximations of  $K_P$  and  $K_T$  can be found in Appendix E.

The composition correction factor has been obtained for three different compositions, which have been classified depending on the methane content. Table 10 presents the reference compositions representing the three possible classifications of the gas richness.

**Table 10.** Reference compositions and KC definition depending on the gas richness

Component	Lean	Medium	Rich
Methane	0.974	0.92	0.87
Ethane	0.0124	0.068	0.062
Propane	0.0045	0.003	0.04
Butane	0.0019	0.002	0.021
Pentane	0.00	0.00	0.00
Nitrogen	0.0072	0.007	0.007
KC	1.05	1	0.89

The data curves and points represented by the obtained correction factors are shown in Figure 13.

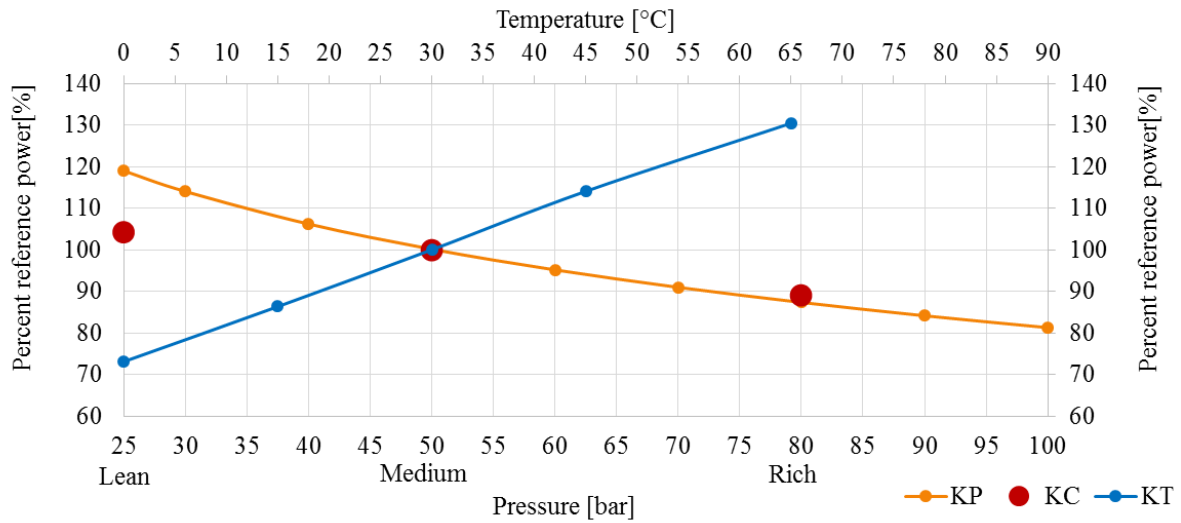


**Figure 13.** Graph representing the effect of the pressure, temperature and composition on the work consumption. Each line represents the percentage variation of the work consumption depending on each parameter.

### Model expression

After obtaining the efficiencies and the correction factors, Equation [3.14] has been obtained to calculate the power needs of the liquefaction drivers. This equation, as for the efficiency expression, is consistent with the mass flow rate at the liquefaction unit inlet.

$$\dot{W}_{Liq} [kW] = \frac{\dot{m}_{Liq} * \Delta e_{reference} * K_P * K_T * K_C}{\eta_{exergy}} \quad [3.14]$$

Where:

- $\dot{W}_{Liq}$  [kW] is the power consumption of the liquefaction drivers
- $\dot{m}_{Liq}$  [kg/h] is the gas flow rate at the inlet of the liquefaction unit model
- $\eta_{exergy}$  is the exergy efficiency of the chosen process type
- $\Delta e_{reference} = 497$  [kJ/kg] is the reference reversible work at 50 bar and 30 °C for medium gas richness

Based on Equation [3.14], the specific power for the process types available in the model, at reference conditions, is presented in **Table 11**.

**Table 11.** Specific power based on the reference conditions, for a medium gas richness.

Process type	Specific power [kWh/ton LNG]
AMR/C3MR	307
SMR	337
N <sub>2</sub> expander	431



### 3.4.6 End flash

For this model, it has been assumed that the flash gas is used for fuel gas. It may be the case that the fuel gas needs are higher than the End flash flow rate, in which case fuel gas should be taken for instance from the BOG or regasifying LNG. This would complicate the GHV calculation due to the different gas compositions, and to simplify, it has been assumed that the End flash gas is sufficient to cover the gas turbine needs.

The End flash model has been defined to allow a maximum of 1 mol% nitrogen in the final LNG product. Figure 14 presents the flow diagram followed to calculate the nitrogen split ratio.

The End flash split ratio is based on the N<sub>2</sub> content in the gas after the liquefaction model. If the N<sub>2</sub> content is lower than 1 mol%, all the N<sub>2</sub> is assumed to be contained in the final LNG product. If the N<sub>2</sub> content is higher, 1 mol% of the N<sub>2</sub> is maintained in the final LNG product, whereas the excess N<sub>2</sub> is assumed to be removed by the End flash. As the fuel is supposed to be taken from the End flash, it is assumed that there is gas flashed even though an End flash is not necessary because the LNG product fulfills the N<sub>2</sub> mol% specification after the liquefaction unit.

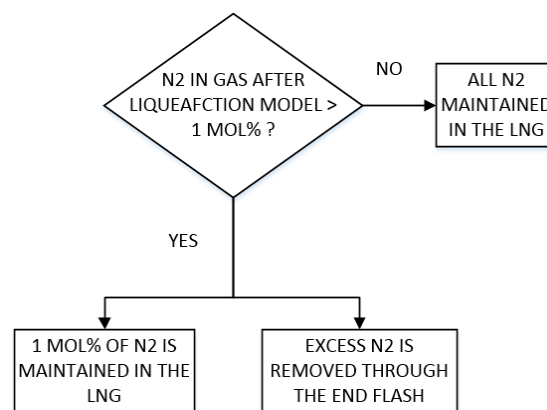


**Figure 14.** Flow diagram for the N<sub>2</sub> Mass balance calculation.

A simulation with HYSYS was performed to obtain the composition of the flash gas and enable the calculation of the GHV for the fuel gas. During the simulation, it was assumed that the liquefied gas after the expansion was at 1.1 bar and bubble point temperature for the reference composition. This gas entered a flash to separate the vapor and liquid phase. The C<sub>1</sub> was varied from 85 to 98 mol% for different nitrogen mol fractions in order to analyze the effect it had in the flash gas composition. The remaining liquid was approximated to ethane, as it was acknowledged that there was no variation between choosing C<sub>2</sub>, C<sub>3</sub> or C<sub>4</sub> because it all remained

at liquid phase. Figure 15 presents the C<sub>1</sub> mass fraction in the flash gas depending on the C<sub>1</sub> and nitrogen content of the liquefied gas at the inlet of the End flash model.

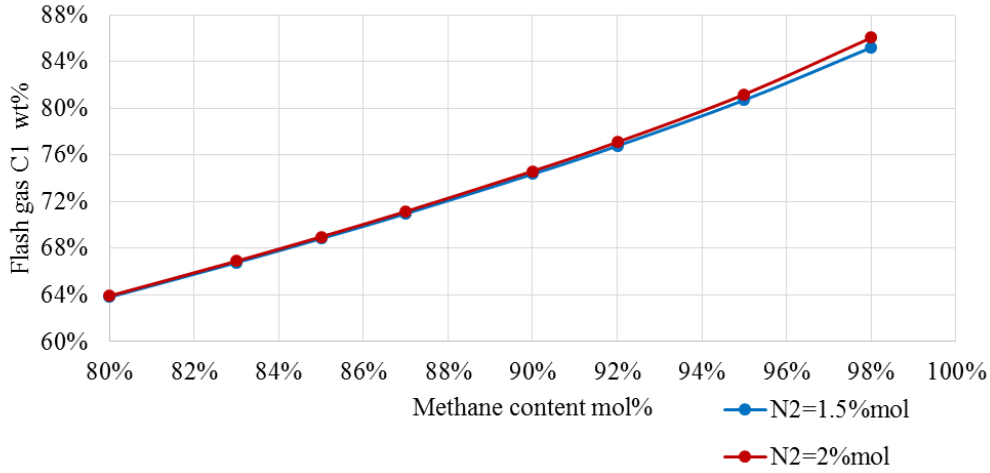


**Figure 15.** Flash gas mass percentage relative to the total gas flow rate, as a function of the C<sub>1</sub> and N<sub>2</sub> in the liquefied gas.

It can be observed that the higher the C<sub>1</sub> content in the liquefied gas is, the higher the concentration of C<sub>1</sub> in the gas flashed. The effect of the nitrogen mol% variation in the inlet gas has been also analyzed. It can be seen in Figure 15 that both curves, representing different nitrogen contents in the liquefied gas entering the End flash, provide a similar methane mass fraction in the flash gas. Thus, it has been assumed that the N<sub>2</sub> content variation in the liquefied gas entering the End flash model is negligible.

Assuming that the flash gas only contains C<sub>1</sub> and nitrogen, it is possible to obtain the GHV of the flash gas, and thus the fuel gas needs. Equation [3.15] defines the content of C<sub>1</sub> in the flash gas as a function of the C<sub>1</sub> mol% in the gas entering the model based on the curves presented in Figure 15. The function has been approximated to a polynomial expression because a linear approximation implied deviations that could easily be avoided by the polynomial one.

$$C_{1,flash} [\%wt] = 1.9(C_{1,liquefied})^2 - 2.2C_{1,liquefied} + 1.2 \quad [3.15]$$

Where  $C_{1,flash}$  is the mass fraction in the flash gas and  $C_{1,liquefied}$  the mol fraction in the gas at the inlet of the model.

The GHV has been calculated on a mass basis to enable the calculation of the fuel gas flow rate through Equation [3.16].

$$GHV_{gas} \left[ \frac{kJ}{kg} \right] = \sum_{i=1}^N w_i * GHV_i \quad [3.16]$$

Where:

- $w_i$  [% kg] the mass fraction of the component  $i$
- $GHV_i$  [kJ/kg] is the ideal mass calorific value of the component  $i$  at 25 °C [8]

Further discussion of the fuel gas calculation can be found in Section 3.4.9.

### 3.4.7 Total power and heat duty calculations

#### Total power consumption

To account for the total electrical consumption of the systems that were not modelled, the work obtained from adding power needs for the liquefaction unit and the amine solution pump in the GSU has been increased by 30%. This scaling was obtained after analyzing different reference cases [2] and evaluating the model accuracy for different percentages. A list of the main systems that are included within this parameter are listed below:

- Compression systems: Condensate, off-gas, LPG, BOG, Flash/fuel gas
- Pumping systems: Cooling system, LNG loading, booster pumps, hot oil, reflux pumps, air compressors, and FLNG thrusters.
- Administration office facilities

Equation [3.17] defines the total power consumption in the LNG plant, which includes both the power needs of the liquefaction unit and the electrical power of the plant.

$$\dot{W}_{total} = 1.3(\dot{W}_{Liq} + \dot{W}_{Amine\ pump}) \quad [3.17]$$

#### Heat consumption

To account for the heat needs of the systems that were not modelled, the heat duty obtained from the addition of the GSU and dehydration unit heat duties has been increased by 20%. This scaling was obtained after analyzing the information available from the reference cases [2]. A list of the main systems that are included within this parameter are presented below:

- Preheaters: Air intake of the gas turbines, GRU unit
- Condensate stabilization
- NGL fractionation: de-propanizer, de-butanizer
- Fuel gas heater

Equation [3.18] defines the total heat duty of the LNG plant.

$$\dot{Q}_{Total} = 1.2(\dot{Q}_{GSU} + \dot{Q}_{Dehydration} + \dot{Q}_{de-ethanizer}) \quad [3.18]$$

### 3.4.8 Drivers

Three different drivers are considered for this model: LM6000 representing aeroderivative turbines, Frame 7 representing the heavy-duty turbines and electrical motors powered by the electrical grid. For the turbine models, the thermal efficiency of each type has been defined and corrected depending on the ambient air temperature. For the electrical motors, a CO<sub>2</sub> emissions factor has been defined for different power systems.

#### Efficiency calculation of gas turbines

The efficiency of the gas turbine will only reflect the effect of the ambient air temperature variation. Therefore, it will not account for other possible losses due to ageing, fouling...etc. Then, the expression for the modified efficiency as a function of the ambient air temperature is:

$$\eta_{GT} = \eta_{GT,design} * f(T) \quad [3.19]$$

Where  $\eta_{GT,design}$  is the efficiency of the turbine at design point.  $f(T)$  is a function of the air ambient temperature which has to be introduced in °C.

The temperature variance of the model has been constrained to temperatures above 0 °C. In case the temperature is lower, the model assumes the same efficiency as for 0 °C. Besides,  $f(T)$  has been assumed linear for both turbine models.

#### LM6000

The LM6000 has been characterized with a  $\eta_{GT,design}$  of 38%. Figure 16 presents the efficiency variation of the LM6000 as a function of the ambient air temperature.

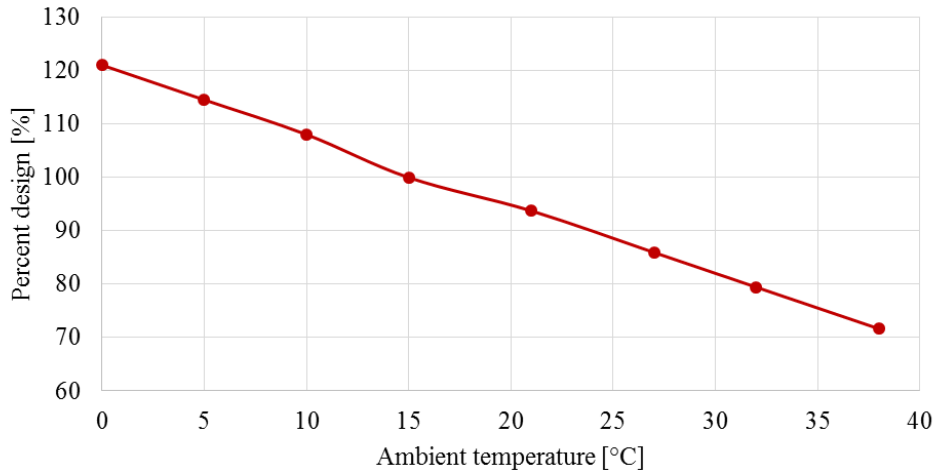


**Figure 16.** LM6000 efficiency at different ambient temperature (adapted from [9]).

This function has been approximated by Equation [3.20] in order to implement this variation on the spreadsheet model.

$$f(T) = (-1.3T + 121)/100 \quad [3.20]$$

### Frame 7

The Frame 7 has been characterized with a  $\eta_{GT,design}$  of 28%. Figure 17 presents the efficiency variation of the Frame 7 as a function of the ambient air temperature.

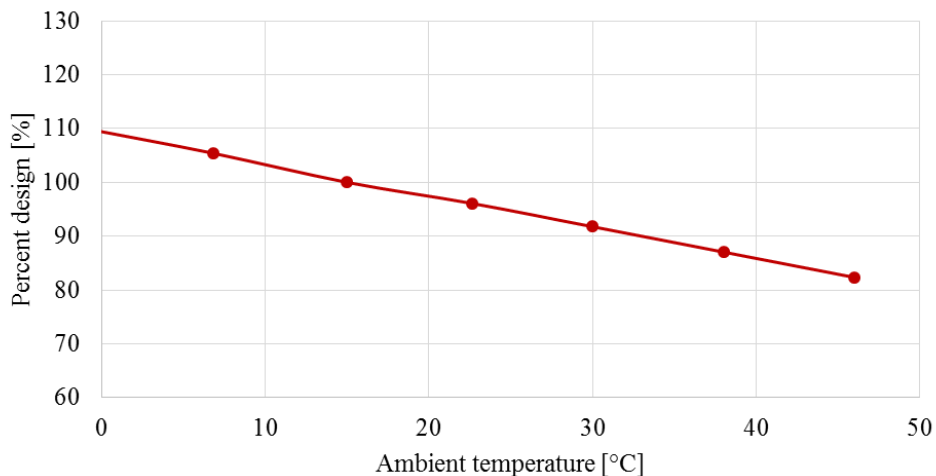


**Figure 17.** Frame 7 efficiency at different ambient temperature (adapted from [10]).

As for the LM6000, the function defining the efficiency has been approximated to Equation [3.21].

$$f(T) = (-0.59T + 109.4)/100 \quad [3.21]$$

## Electrical grid

The larger availability of the electrical grid, as well as the emissions reduction, has increased the interest of providing new LNG plant projects with power from it.

The electrical grid has been defined to partly or fully cover the needs of the plant. Depending on the desired ratio between the gas turbines and the electrical grid usage, the fuel gas calculation and the CO<sub>2</sub> emissions are calculated consequently. The electrical grid is assumed to only cover the electrical needs of the plant, whereas the heating needs are covered by the combustion of fuel gas. In case gas turbines and the grid are used simultaneously, the waste heat from the gas turbines is assumed sufficient to cover the heating needs.

The CO<sub>2</sub> emission estimations are obtained based on the configuration of the plant. A CO<sub>2</sub> emissions estimation based on the fuel gas combustion can be found in Section 4.3.5, whereas a CO<sub>2</sub> emissions factor to account for the electrical power consumption from the grid has been described below.

Two different options have been addressed in the model: electricity imported from a local station, and electricity from the region electrical grid.

For the local station case, it has been necessary to obtain an estimation of the CO<sub>2</sub> depending on the type of power generation plant that provides the electricity. For this task, three different types of power plants have been defined: combined cycle plant, coal fired plant and renewable energy plant. Typical CO<sub>2</sub> emissions have been obtained from reference data [11, 12]. The CO<sub>2</sub> estimation is assumed to be an approximation because the values obtained can vary largely depending on individual conditions of each plant and the local climate. Table 12 presents the CO<sub>2</sub> emissions per electrical MJ consumed in the LNG plant.

**Table 12.** Definition of the efficiencies for each one of the power plants types, and scaling factor for estimation of the CO<sub>2</sub> emissions for each one.

Plant Type	CO <sub>2</sub> emissions [kg/MWh]
Combined cycle	360
Coal fired	740
Renewable	0

For the case in which the electricity is taken from the regional grid, no assessment has been performed because of the large range of possibilities. Therefore, the emissions factor for this option must be provided as an input in order to estimate the emissions.

### 3.4.9 Fuel gas calculation

A fuel gas model has been necessary to account for the gas taken to produce the required power. The model calculates the amount of fuel gas necessary for the total power production, as well as the final LNG production after the End flash gas removal.

One of the main issues during the model design was the decision of where the fuel gas would be taken from. Figure 18 shows a typical fuel gas balance in an LNG plant. It is usual to get the End flash gas, the BOG from tanks and the ship vapor return in order to supply the gas turbines with fuel. However, sometimes the flash gas may not be sufficient, or it may not be valid as a fuel gas due to its high nitrogen content that might make it unsuitable for the gas turbines. Besides, the BOG and ship vapor return, fixed by design, often are not sufficient by themselves to cover the fuel needs. An alternative option is to take the gas after the slug catcher, but this option is not as widely used as for the other cases, being commonly used only for startup of the plant.

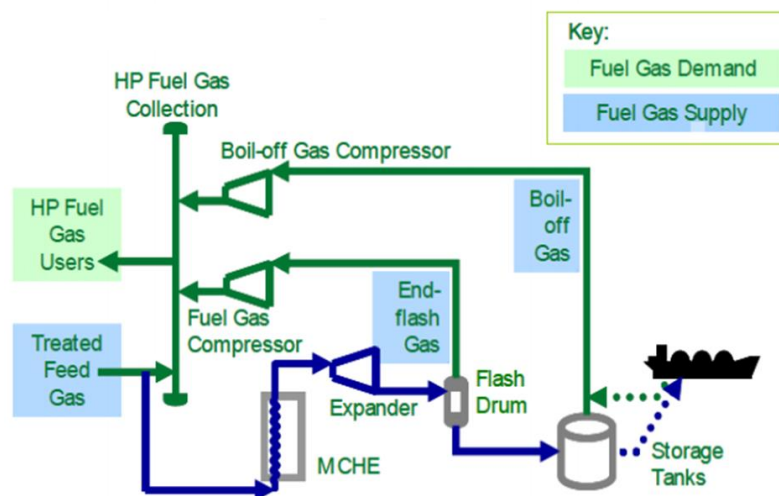


**Figure 18.** Typical fuel gas balance in LNG plants (source: BP).

Due to the spreadsheet limitations, it was too complex to implement a model that obtained the fuel gas from all the different possibilities. It has been decided to use the End flash intake due to its more extended use and availability than the other options (see Appendix F for upstream fuel gas intake alternative). BOG and ship vapor return were considered to contribute to some extent to the End flash gas intake, but it was finally discarded due to the complexities it entailed.

The model then assumes that fuel gas is only taken from the End flash. Once the End flash gas composition is obtained through Equation [3.15], and thus the GHV of this gas calculated, it is possible to estimate the fuel gas flow rate that is necessary to run the gas turbines through Equation [3.22].

$$\dot{m}_{fuel} \left[ \frac{ton}{h} \right] = \frac{\dot{W}_{GT}}{GHV * \eta_{GT}} \quad [3.22]$$

Where:

- $\dot{m}_{fuel}$  [kg/s] is the fuel gas consumption
- $\dot{W}_{GT}$  [MJ/kg] involves all the power needs of the LNG plant covered by the gas turbines.
- $GHV$  [MJ/kg] is the e Gross Heating Value of the End flash gas
- $\eta_{GT}$  [-] is the efficiency of the gas turbine

In case the electrical grid is used, Equation [3.22] must be specified for the total heat duty instead of the power needs.

Once the fuel gas flow rate has been calculated, it is possible to estimate the amount of CO<sub>2</sub> emitted due to the combustion of this fuel gas. As the End flash is assumed to only contain methane and nitrogen, and the latter does not contribute to the emissions, a very simple reaction has been defined in Equation [3.23] to obtain the CO<sub>2</sub> from the combustion.



The mol flow rate of methane in the fuel gas is obtained from the fuel mass flow rate, and then the amount of CO<sub>2</sub> produced can be obtained through the reaction defined above.



## 4 MODEL TESTING

The model has been tested against six different real cases [2]. All these cases provide information about the liquefaction power, the LNG, LPG and Condensate production, and the CO<sub>2</sub> emissions from the feed and from the total power consumption and heat generation. Besides, two different cases provide further information about the electrical power and heating needs of different units, the fuel gas consumption and the total power consumption and heat duty.

A comparison of the production rates, liquefaction power needs and CO<sub>2</sub> emissions has been performed and compared for all the cases. Besides, the remaining estimations have been compared against the available data.

The results have been expressed as the relative error of the estimation with respect to the reference data. The numerical data of all the comparisons is summarized in Appendix G.

### 4.1 Reference cases

#### Benchmarking data

The reference data [2] for benchmarking is presented in the present section. Table 13 presents the plant parameters, Table 14 the feed gas and process parameters and Table 15 and feed gas composition. Besides, Table 16 and Table 17 provide the different data that has been compared to the model estimations.

**Table 13.** Main Plant parameters of the benchmarking cases.

Plant parameters	Case A	Case B	Case C	Case D	Case E	Case F
Type of plant	FLNG	Onshore	Onshore	FLNG	FLNG	FLNG
Compressor drivers	Aero GT	Aero GT	Industrial GT	Aero GT	Aero GT	Aero Gt
Cooling method	Water	Water	Air	Water	Air	Air
Nominal capacity	3.3	4.3	13.5	3.1	4.4	4
Process type	AMR	AMR	C3MR	AMR	SMR	N <sub>2</sub> expander

The flow rate in case C is originally given in Sm<sup>3</sup> per year. To perform the calculations it was necessary to provide a flow rate in mass basis, and to do that the density has been calculated for standard conditions, and the flow rate has been calculated for a yearly production of 350 days, consistent with the number of production days later used for onshore LNG plants.

**Table 14.** Main feed gas and process parameters of the benchmarking cases.

Feed gas and process parameters	Case A	Case B	Case C	Case D	Case E	Case F
Flow rate [ton/h]	615	816	1800	474	638	533
Arrival pressure	67	70	70	67	55	70
Mean cooling water temperature °C	14	7.0	-	12.0	-	-
Mean air temperature, °C	27.3	7.0	23.0	28.0	30.0	27.0

**Table 15.** Feed gas composition in mol percent of the benchmarking cases.

Feed gas composition, % mol	Case A	Case B	Case C	Case D	Case E	Case F
Methane	79.8	80.5	97.7	96.5	95.1	94.3
Ethane	4.3	5.1	1.3	1.2	2.8	0.6
Propane	1.5	2.6	0.3	0.4	0.3	3.4
n-Butane	0.3	0.8	0.1	0.1	0.1	0.1
i-Butane	0.4	0.5	0.1	9.1	0.0	0.1
n-Pentane	0.2	0.5	0.0	0.0	0.0	0.3
i-Pentane	0.2	0.5	0.0	0.0	0.0	0.2
C6+	3.0	1.8	0.1	1.0	0.2	0.1
Nitrogen	0.9	2.5	0.2	0.7	0.2	0.1
Carbon dioxide	9.4	5.2	0.2	0.0	1.3	0.8

Table 15 presents the reference data that has been compared against the model estimations. For the production of each product, it has been necessary to assume a number of operation days. For the FLNG plants the operation days was set to 330 days, whereas for the onshore plants it was set to 350. Only one of the six cases produces LPG, and it has not been possible to validate the model for this product.

**Table 16.** Reference values for liquefaction power, mass balance and CO<sub>2</sub> emissions.

Parameter	Case A	Case B	Case C	Case D	Case E	Case F
Liquefaction power, MW	125.0	162.0	660.0	124.0	196.0	225.0
LNG production, Mtpa	3.3	4.2	13.5	3.1	4.1	3.6
LPG production, Mtpa	0	0.3	0.0	0.0	0.0	0.0
Condensate production, Mtpa	0.3	0.7	0.3	0.05	0.01	0.2
CO <sub>2</sub> from feed, tpa	995,000	640,000	120,000	23,000	150,000	83,000
CO <sub>2</sub> from power and heat generation, tpa	797,000	900,000	3,700,000	820,000	1,355,000	990,000

Table 17 presents the additional reference data that was compared to the model estimations. Each model provided information about different parameters, and these values were used to analyze the accuracy of the model.

**Table 17.** Reference values for work and heat balance for cases A and B.

Parameter	Case A	Case B
<b>Work balance</b>		
Total power consumption, MW	180	218
MDEA pump power, MW	5.1	3.3
Fuel gas, ton/h	42	40
<b>Heat balance</b>		
Total heat duty, MW	138	147
MDEA solution regenerator heat duty, MW	96	63
Gas dehydration Unit heat duty, MW	3.8	8.9
De-ethanizer heat duty, MW	15.45	7.5

## 4.2 Testing results for the six cases

The results have been split depending on the estimated parameter. Afterwards, All the cases have been grouped and analyzed to study the overall model performance. Table 18 contains the model results for the six cases. These are the estimations that have been compared to the reference data stated in Table 16.

**Table 18.** Model results used for benchmarking of the six cases.

Benchmarking results	Case A	Case B	Case C	Case D	Case E	Case F
Liquefaction power, MW	117.4	156.2	585.7	128.6	250.0	241.7
LNG, Mtpa	3.0	4.6	13.1	3.2	4.2	3.4
LPG, Mtpa	0	0.25	0	0	0	0
Condensate, Mtpa	0.62	0.72	0.08	0.19	0.05	0.11
CO <sub>2</sub> from feed, tpa	898,588	725,906	80,454	0	169190	83738
CO <sub>2</sub> from liq. drivers, power/heat generation, tpa	690,563	732399	4,245,612	732422	1,473,602	1,358,925

### 4.2.1 Liquefaction power

Figure 19 shows the discrepancy between the liquefaction power of the reference data and the obtained model estimations.

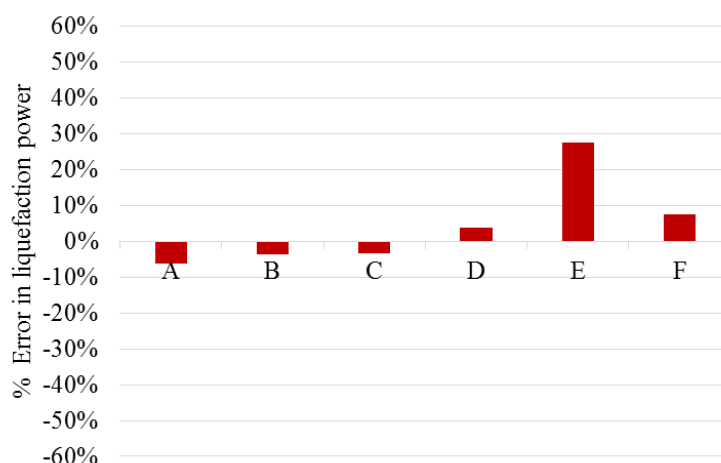


**Figure 19.** Relative error percentage in liquefaction power for the six cases.

The model has demonstrated a correct estimation of the liquefaction power. Case E presents the largest relative error of +28% with respect to the reference data, which is well above the rest of the cases, presenting deviations lower than +/-10%.

The possible source of error for case E was analyzed. This case is the only one using Single Mixed Refrigerant process type. The liquefaction power was recalculated using the AMR efficiency instead, to see if the efficiency set for the SMR process type was wrong. For the AMR efficiency, the relative error decreased to +21%. This estimation is still above all the remaining cases, and therefore this analysis concludes that the efficiency definition of the SMR process type is not the source of error of this case, ignoring then the reason why this liquefaction power error is that large.

#### 4.2.2 LNG production

Figure 20 shows the discrepancy between the reference LNG production data and the model estimations.

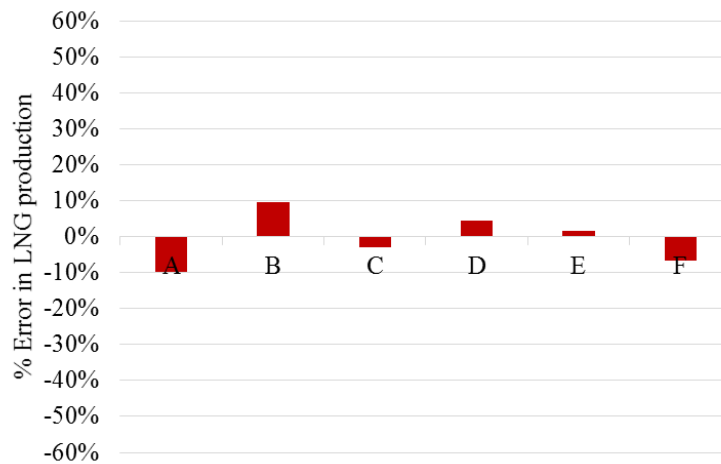


**Figure 20.** Relative error percentage in LNG production for the six cases.

The LNG production has been accurately approximated for the six cases. All of them have presented a relative error lower than +/-11%.

#### 4.2.3 LPG production

Figure 21 presents the discrepancy between the reference LPG production data and the model estimations. This estimation only accounts for case B because the LPG production data was zero in the rest of the reference cases.

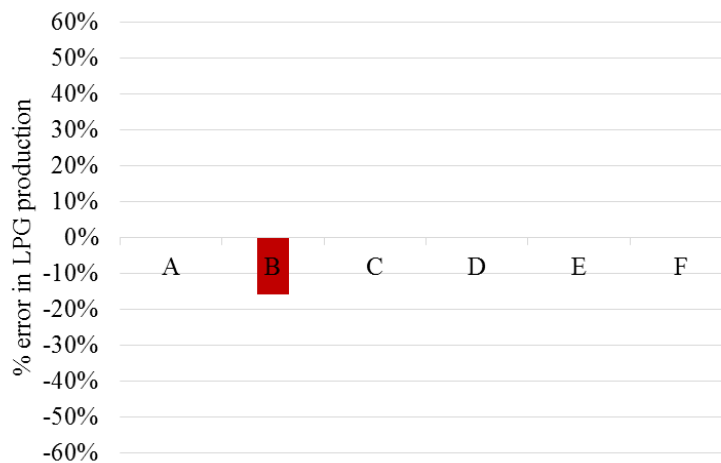


**Figure 21.** Relative error in the LPG production for case B.

For the only case analyzed, the LPG production estimation presents a relative error -16%. This result correctly approximates the production rate of the reference data, but more reference cases should be compared in order to validate the model. The different split ratios modelled to reflect the LNG richness in the extraction unit model have to be improved.

#### 4.2.4 Condensate production

Figure 22 presents the discrepancy between reference Condensate production data and the model estimations.

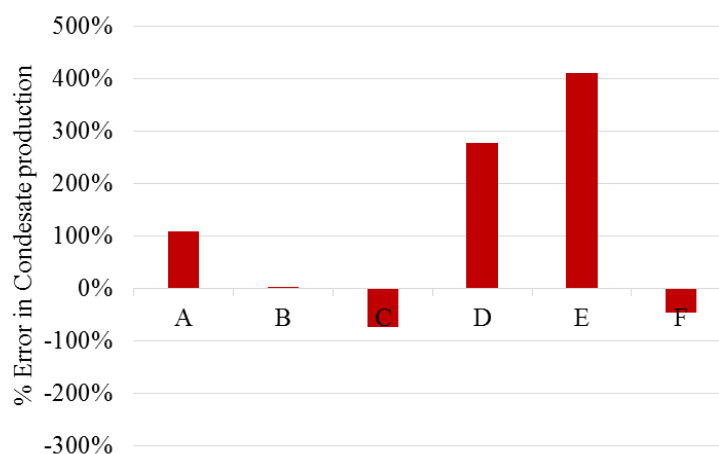


**Figure 22.** Relative error percentage in the Condensate production for the six cases.

For this estimation, only case B provides a valid result of the Condensate production. The model was defined to produce all the C<sub>5+</sub> content as Condensate, and this simplification did not correctly estimate the total Condensate production. An overestimation of the Condensate production can be explained by the simplification stated above, but it has not been found a reason why there is an underestimation for cases C and F. The molecular weight simplification for the C<sub>6+</sub> can lead to high deviations in case the real mean molecular weight differs largely from the C<sub>6</sub>, and the increase of the accuracy during the calculation of the mean molecular weight might decrease the deviation in the underestimation cases, but this possible decrease does not justify the deviation of both cases.

#### 4.2.5 CO<sub>2</sub> emissions from feed gas

Figure 23 presents the relative error of the estimation of CO<sub>2</sub> emissions due to its removal in the GSU unit. Case D has not been compared because the provided composition does not present any CO<sub>2</sub> content.

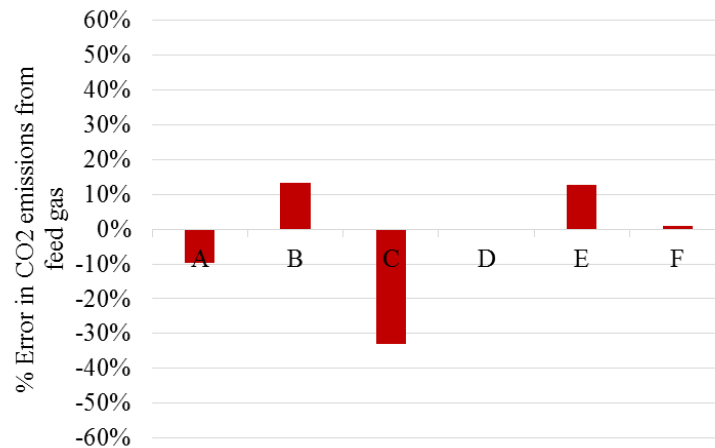


**Figure 23.** Relative error percentage in the CO<sub>2</sub> emissions from feed for the six cases.

The model has presented a close agreement with the assumption made. Due to the strict requirements in the LNG, it was assumed that all the CO<sub>2</sub> in the feed gas was removed. The estimation in case C presents a relative error of -33%, but for this case the mass flow rate was also approximated for an assumption of 350 production days per year. If the production days are assumed to be 330 days instead, the flow rate per hour increases from 1800 ton/h to 1909 ton/h, and the relative error of this CO<sub>2</sub> emissions estimation decreases to -29%. Therefore, the estimation for case C has been accepted as valid.

#### 4.2.6 CO<sub>2</sub> emission from liquefaction drivers, electrical power and heat generation

Figure 24 presents the estimation of the CO<sub>2</sub> produced due to the liquefaction drivers, electrical power and heat generation.

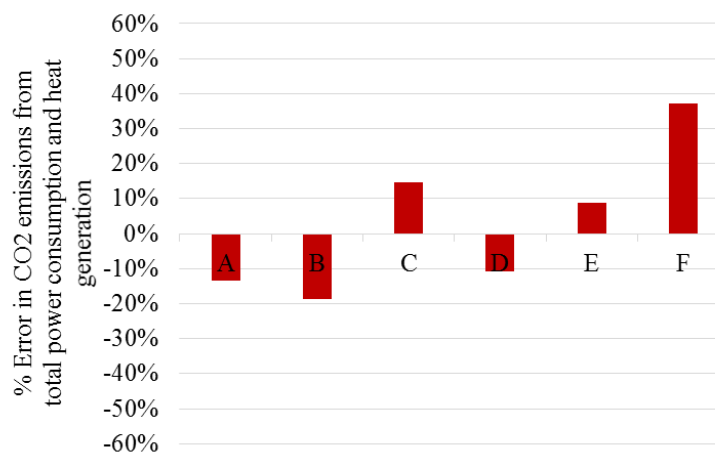


**Figure 24.** Relative error percentage in the CO<sub>2</sub> emissions from the liquefaction drivers, electrical power and heat generation for the six cases.

The simplified model has shown to be an accurate estimation for the CO<sub>2</sub> emissions, with a relative error range between -19% and +37%. Case F appears to be the only one exceeding the limit of +/-30%, and it has been analyzed to find the source of this deviation.

Cases A and F have been compared using the available data to analyze the validity of the reference data CO<sub>2</sub> emissions for case F. Both cases are FLNG plants and use aeroderivative turbines, and their total power consumption are available for comparison. In case A, the kg of CO<sub>2</sub> emitted per MWh generated is 576 kg/MWh, whereas for case F is 432 kg/MWh. This implies a relative difference of -25% with respect to the emissions of case A. The CO<sub>2</sub> emissions for case F using 576 kg/MWh results in 1,244,205 tpa, what implies a relative deviation of the model estimation of -9%, a result much closer than the reference data provided for case F. This analysis concludes that the real CO<sub>2</sub> emissions from the power and heat generation in case F could be higher than the value provided.

#### 4.2.7 Validation of the cases

Figure 24 presents the results grouped by case to analyze the validity of the model. The Condensate production estimations have been discarded. Disregarding the unrepresentative results discussed above, the model has provided estimations with deviations well below the maximum tolerated of +/- 30% for all the cases.

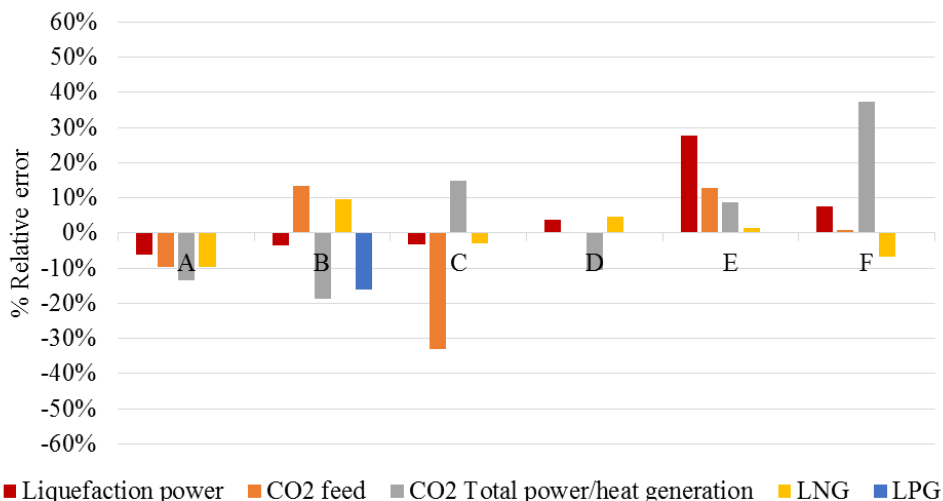


**Figure 25.** Results summary for the six different cases.

The model has demonstrated to provide valid estimations for the liquefaction power, the LNG production, and the CO<sub>2</sub> emissions. Cases A and D present the most accurate results with



a relative error within +/-13% in all the estimations presented. The CO<sub>2</sub> estimation from the feed in case C has to be further studied, as it is the only estimated parameter within the four representative parameters for this case that presents an unusual deviation with respect to the reference data.

### 4.3 Testing results for cases A and B

Cases A and B have been additionally tested for the total power and heat duty consumption, MDEA solution pump power, dehydration duty, de-ethanizer reboiler duty and fuel gas flow rate. Table 19 presents the additional model results for the six cases. These estimations have been only compared to the available data from cases A and B, whereas the others have been commented in case unusual estimations were obtained.

**Table 19.** Additional model results for the six cases.

Benchmarking results	Case A	Case B	Case C	Case D	Case E	Case F
Total power, MW	159.3	208.4	762	167.2	326.0	314.9
Total heat duty, MW	143.7	132.6	109.1	12.6	68.8	208.4
MDEA solution regenerator, MW	98.3	74.9	8.3	0	18.5	9.2
MDEA solution pump, MW	5.2	4.1	0.46	0	0.8	0.5
De-ethanizer, MW	13.7	31.2	11.1	3.7	3.8	140.8
Dehydration, MW	7.8	4.4	71.15	6.8	35.0	23.6
Fuel gas flow rate, ton/h	46.8	49.2	220.2	41.2	84.5	85.2
Fuel gas GHV [kJ/kg]	37700	35580	46434	45400	44512	40745

#### 4.3.1 Total power and heat duty

Figure 26 presents the relative error percentage of the total power and heat duty with respect to the reference data.

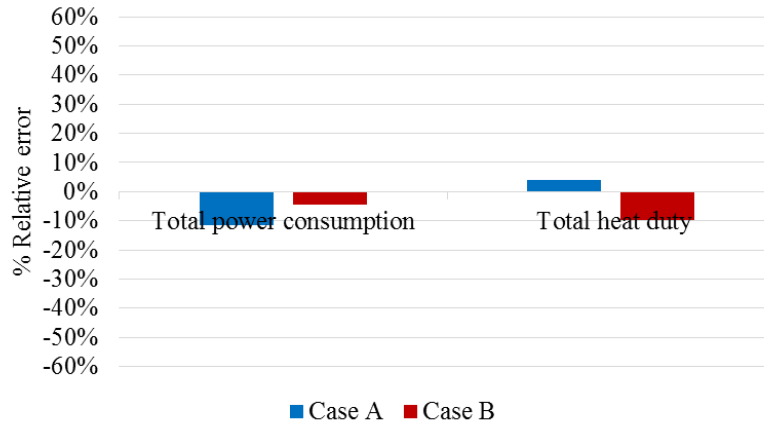


**Figure 26.** Relative error percentage in the Total electrical power and heat duty.

The total power and heat duty present a deviation between -12% and +4%. The scaling factors used for these estimations were defined after analyzing the two cases, showing a close agreement for both of them.

Besides, the results of all the remaining cases have been analyzed, and it has been observed that low CO<sub>2</sub> content in the gas leads to a very low CO<sub>2</sub> regenerator duty, and as the total heat duty is scaled from it, this low values lead to very low total heat duty that should be revised.

#### 4.3.2 MDEA solution pump and regenerator

Figure 27 represents the relative error percentage of the GSU model, that entails the MDEA solution regenerator heat duty and pump power.

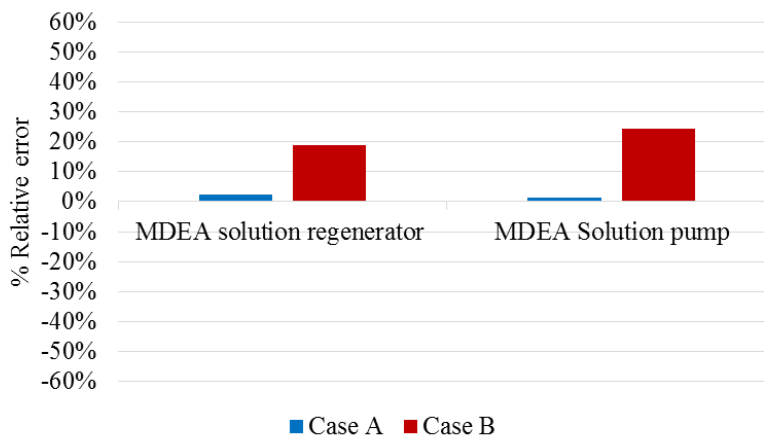


**Figure 27.** Relative error percentage in the MDEA solution regenerator and pump power model.

The CO<sub>2</sub> regenerator and solution pumps have shown to accurately estimate their respective values. Case A presents a negligible deviation for both, whereas case B has presented larger deviations, always below the maximum deviation accepted.

According to the Total heat duty estimation for the rest of the cases, the MDEA solution regenerator and pump model provides very low heat duties. These results have to be compared in order to analyze whether the model is valid for low CO<sub>2</sub> content feed gas or not.

### 4.3.3 Dehydration

Figure 28 shows the relative error percentage of the dehydration model with respect to the reference data.

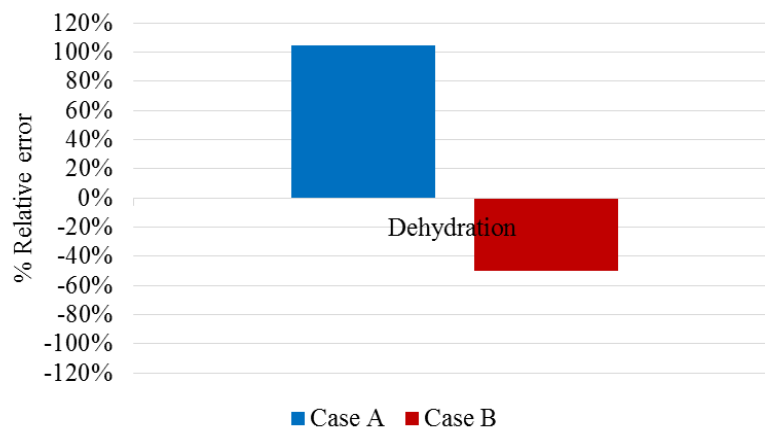


**Figure 28.** Relative error percentage in the dehydration heat duty model

The dehydration unit has presented relevant deviations. Case A presents a deviation of +104% relative to the real data, whereas case B relative deviation is -50%. The reference analysis [6] was only based on two different pressures and temperatures, and this thesis work assumed the dependence of the heat duty with respect to these parameters to be linear. Therefore, it is necessary a more detailed dehydration model, possibly based on the reference procedure, to define correctly the correction factors that account for the temperature and pressure.

### 4.3.4 De-ethanizer

Figure 29 represents the relative error percentage of the de-ethanizer unit with respect to the reference data. The de-ethanizer model has presented disparities for the two cases. Case A

provides an estimation with a deviation of -12%. On the other hand, case B presents a deviation of +316%, invalidating this model estimation.

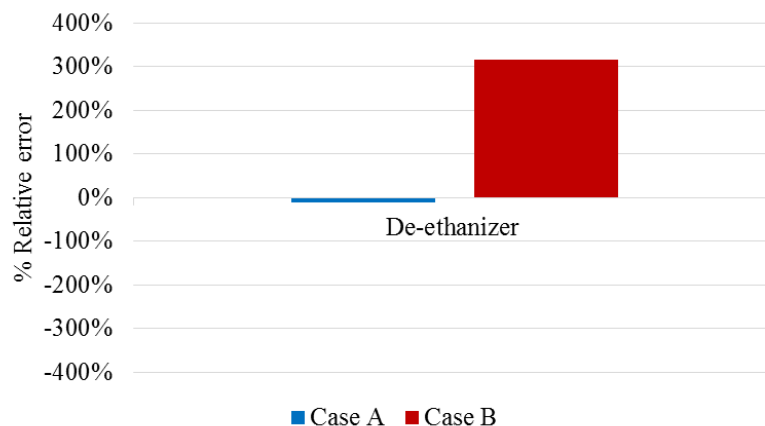


**Figure 29.** Relative error percentage in the de-ethanizer heat duty model.

The model has been analyzed for these two cases. The estimated duty for case A is 13.66 MW and 30.19 MW for the case B. It has been found that the difference derives from the total mass flow rate, and therefore the mass balance definition. The specific heat duty in kWh per kg of gas was similar for both cases, but due to the split ratios defined in the model, as well as the assumption that considers that all the C<sub>2+</sub> flows through the de-ethanizer, case B accounted for a much higher gas flow rate.

It has been observed that the total heat duty for case F appears to be quite high. The specific heat duty in kWh per kg has shown to be 0.26 kWh/kg, what represents twelve times the specific heat duty for cases A and B. This high value has been addressed to the low ratio C<sub>2</sub>/C<sub>3</sub> that appears to be out of the model range.

#### 4.3.5 Fuel gas flow rate

Figure 30 shows the relative error percentage in the model of the fuel gas flow rate with respect to the reference data.

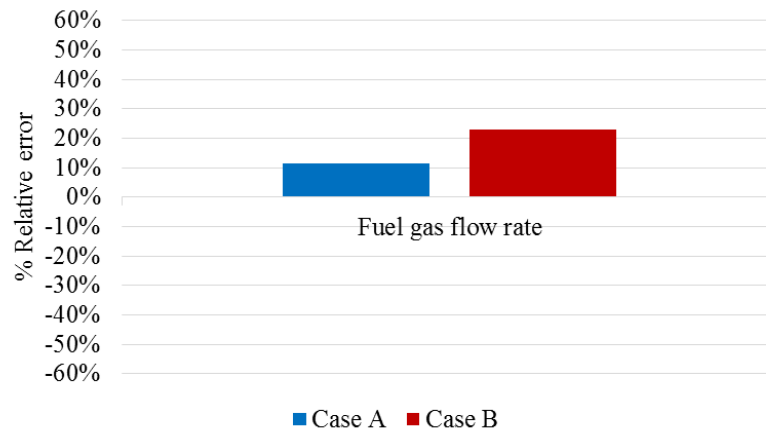


**Figure 30.** Relative error percentage in the fuel gas flow rate model.

The fuel gas flow rate model has provided estimations for both cases which are larger than the real data ones. Case A presents a relative error of +11%, whereas case B presents a +25%. These results validate the simplified model used for the fuel gas calculation



## 5 CONCLUSIONS AND RECOMMENDATIONS

The model has demonstrated to provide accurate estimations through the implementation of simple expressions that correctly defined the processes. The results present a deviation well below the limit established for the LNG production, the liquefaction power and the CO<sub>2</sub> estimations. These estimations have been provided for a wide range of variants, what implies that the model defined presents a reliable tool for calculation of these parameters. Moreover, the LPG production, the Gas Sweetening Unit, the fuel gas flow rate and the scaling factors defined for the total power and heat duty have been correctly estimated. These models have presented as well deviations below the set limits of +/-30%. However, the range has been limited to the available data, and larger deviations could be expected in case the plant evaluated differs from the validated cases.

A summary of the conclusions deduced from the model test are presented:

- Correct estimations have been provided for the liquefaction power, LNG, and CO<sub>2</sub> emissions
- Condensate estimations present deviations over +/- 100% due to the mass balance simplifications in the Separation model.
- LPG production has provided a deviation of -16% that validates the model for the only case compared
- The scaling factor for the total power and heat duty estimations have been validated, providing results with relative error between -12 and + 4%.
- The Gas Sweetening Unit model has correctly defined the MDEA regenerator heat duty and pumping power for CO<sub>2</sub> feed gas content over 5 mol%.
- The dehydration model has to be redefined to correctly calculate the heat duty of this unit.
- The de-ethanizer model assumption regarding the mass flow rate entering the unit has invalidated the model
- The intake of the fuel gas from the End flash has presented accurate results that validate the model simplifications.

## CONCLUSION

Additionally, the following recommendations are suggested based on the conclusions reached:

- A split ratio should be defined to estimate the Condensate production
- The Gas Sweetening Unit should be validated for low CO<sub>2</sub> content feed gas
- A dehydration model, possibly based on the procedure followed in [6] should be created for a better definition of the process
- The LPG split ratio can be further developed to account for more detailed LNG richness definition and LPG production rate. Moreover, more cases with LPG production should be studied to validate the model over a wider range of plant configurations
- The assumptions in the mass flow entering the de-ethanizer model should be redefined, accounting for a more realistic mass flow rate instead of the entire C<sub>2+</sub> content in the feed gas.
- The mass balance implemented in the End flash model can be further developed to provide a better definition of the LNG product composition. This upgrade would lead to an estimation of the GHV of the LNG, improving the basis for the project assessment and economic analysis.
- The fuel gas model should be defined to allow simultaneously different intake options. The fuel gas composition has to be defined in detail in order to obtain more accurate estimations



## 6 REFERENCES

- [1] S. Mokhatab, J. Mak, J. V. Valappil, and D. A. Wood, *Handbook of liquefied natural gas*, First edition. ed. Amsterdam: Elsevier, GPP, 2014.
- [2] J. Petterssen, Senior Specialist, Statoil. Personal Communication, email.
- [3] Y. Bramoullé, "LNG quality and market flexibility challenges and solutions," Total Gas & Power- Technology Division.
- [4] K. Arnold and M. Stewart, *Surface production operations*, 2nd ed. Houston, Tex.: Gulf Pub. Co., 1998.
- [5] Gas Processors Association. and Gas Processors Suppliers Association (U.S.), *Engineering data book*, 12th ed. Tulsa, Okla. (6526 E. 60th St., Tulsa 74145): Gas Processors Suppliers Association, 2004.
- [6] P. Campbell, "What is the Impact of Feed Gas Conditions on the Adsorption Dehydration System?."
- [7] J. D. Bukowski, "Natural Gas Liquefaction Technology for Floating LNG Facilities," ed: Air Products and Chemicals , Inc.
- [8] Y. A. Çengel and M. A. Boles, *Thermodynamics : an engineering approach*, Seventh edition. ed. New York, NY: McGraw-Hill, 2011.
- [9] G. Energy, "LM6000 -50/60 HZ Gas Turbine Generator Set- Product Specification," ed, 2015.
- [10] F. J. Brooks, "GE Gas Turbine Performance Characteristics," GE Power Systems.
- [11] O. Bolland, *Thermal power generation: Norges Teknisk-Naturvitenskapelige Universitet*, 2014.
- [12] I. E. Agency, "Power Generation from Coal," Coal Industry Advisory Board October 2010 2010.



## APPENDIX A: CONDENSATE STABILIZATION MODEL

Appendix A presents the defined model for the estimation of the Condensate stabilization heat duty, that was discarded after the large deviations it presented. For the model, it was assumed that the temperature and pressure did not affect the heating needs of the Stabilization Unit, as it further complicate the model.

Due to the possible range compositions in the feed gas, it was not found a general model that represented the heat duty of all the different possibilities. The heat duty in the stabilization does not only depend on the condensate amount but on its specific composition. It was intended to simplify the composition of the HHC into a single “mean component” and use it to obtain the heat duty needs of the stabilization. It was then made an analysis of the different condensate components’ phase behavior, in order to choose one component that could be representative of the condensate composition. This component had to be removed in liquid state at typical operational parameters of the column, that were decided to be 200 °C and 10 bar. Figure 31 presents the Pressure-Temperature curves of the different components. At this point, C<sub>6</sub> had to be discarded as a representative “mean component” because it did not fulfill the specifications.

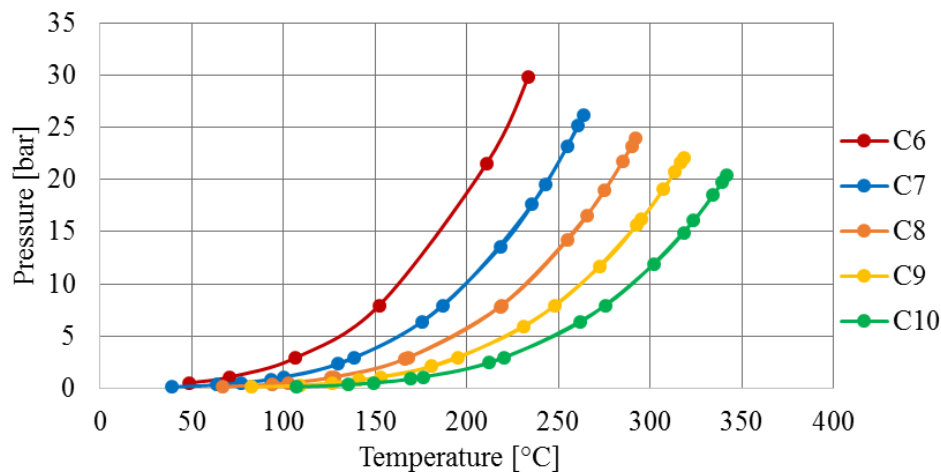


**Figure 31.** Pressure-Temperature diagram of different pure components in the feed gas.

Afterwards, a simple model of the stabilization column was simulated in HYSYS to obtain a heat duty estimation. The model was simulated for a reference case [2], and the condensate composition was approximated to different mean components to study the effect this assumption implied on the heat duty. Figure 32 presents the deviation that each mean component simulation has with respect to the reference case data.

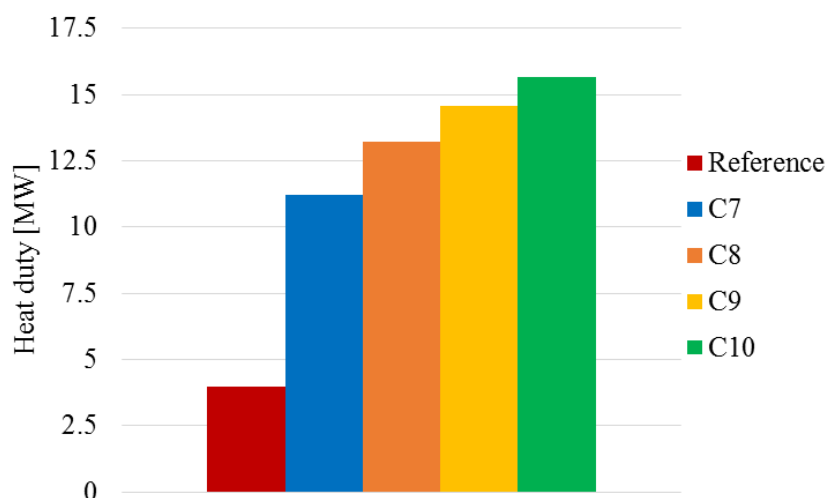


**Figure 32.** Variation of the heat duty for different mean components. The graph shows the relative variation with respect to the C<sub>8</sub> that was decided to be used as mean component.

It was found that the model did not correctly approximated the heating needs of the unit for any of the “mean components”. All of the calculated heat duties differ from the reference value largely. Moreover, the relative error with respect to the reference data varies between +230 and +292% depending on the “mean component” selection. These two facts invalidated the assumptions and simplifications made, and alternatively it was decided to use the scaling factor stated in Section 3.4.7 to account for the heating needs of the condensate stabilization.

## APPENDIX B: GAS SWEETENING UNIT CALCULATIONS

To obtain the pumping power necessary to pump the solution, a model has been developed to obtain the power as a function of the amine mass flow rate and the pressure of the feed gas. The process simulation tool HYSYS has been used for this purpose. An available Amine process for acid gas removal has been used to obtain an expression of the power consumption of the solution pump.

The process has been simulated for a CO<sub>2</sub> content between 2 mol% and 20 mol%, and pressures between 25 and 70 bar, for a constant feed gas inlet temperature of 30 °C. Figure 33 presents the pumping power as a function of the amine mass flow rate.

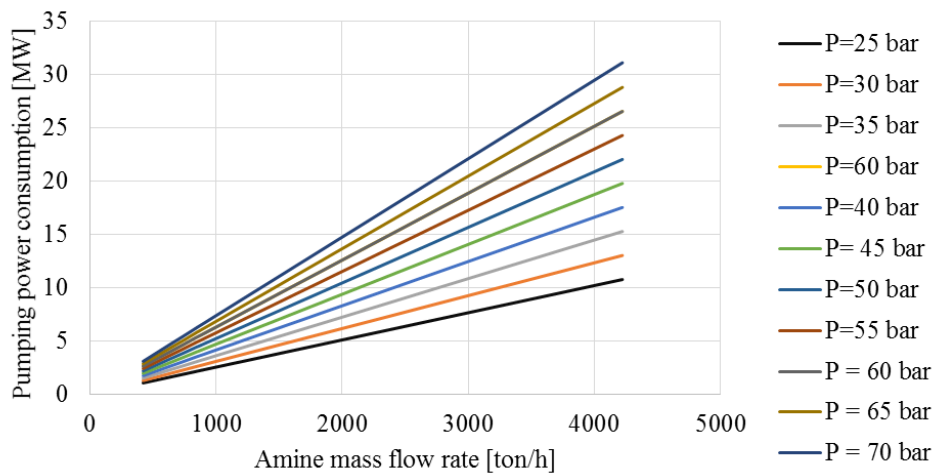


**Figure 33.** Pumping power consumption as a function of the Amine mass flow rate and the feed gas inlet pressure.

All the functions have shown to be linear, and therefore defined by the expression:

$$\dot{W} = a * \dot{m}_{amine} + b \quad [\text{B.1}]$$

The expression for the power consumption has been found to have the form

$$\dot{W} = a(P) * \dot{m}_{amine} + b(P) \quad [\text{B.2}]$$

Where  $b(P)$  has not been taken into account due to its negligible contribution to the function.

The function  $a(P)$  has been approximated to an expression in order to represent the pressure effect on the pumping power consumption. A linear and a logarithmic expressions were tried

to study the accuracy of the final expression, being the logarithmic one more accurate for defining the pressure effect due to the numerous decimals contained in the linear expression.

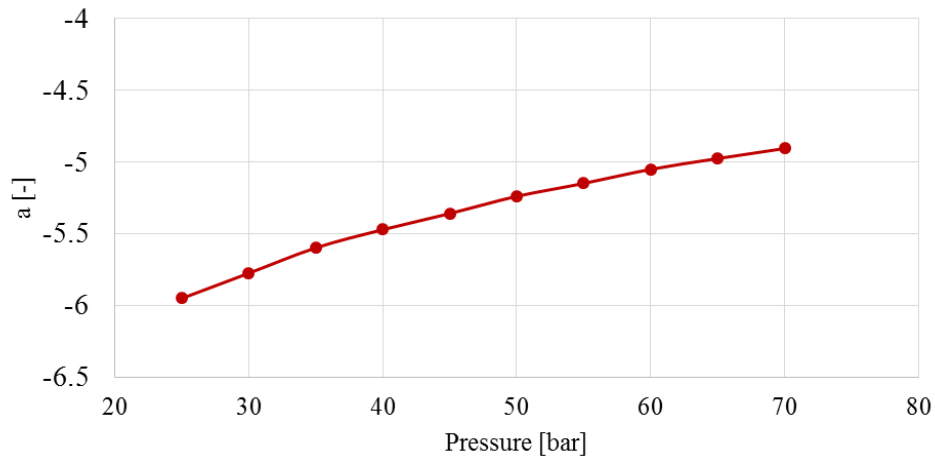


**Figure 34.** Parameter “a” as a function of feed gas arrival pressure.

Finally, the model function has been defined as follows:

$$\dot{W}_{Amine\ pump}[kW] = e^{1.02 \ln(P) - 9.25} * \dot{m}_{amine} \quad [B.3]$$

In order to provide a better representation of the pumping power variation, the information provided in Section 3.4.3 has been expressed as a function of the CO<sub>2</sub> in the feed gas instead of the amine flow rate. Besides, this power need has been tested for values of the pressure up to 100 bar with successful results, enabling the model to work under this pressure level.

## APPENDIX C: DEHYDRATION UNIT CALCULATIONS

The calculation of the heat duty in the dehydration process has been subjected to different simplifications that were necessary due to its complexity when it comes to obtain all the different parameters of the process. The different factors has been obtained under the conditions stated in [6]. Figure 35 presents the heat duty variation depending on the gas flow rate, temperature and pressure. These results from the reference case have been used to characterize the expressions used in the dehydration model of this report.

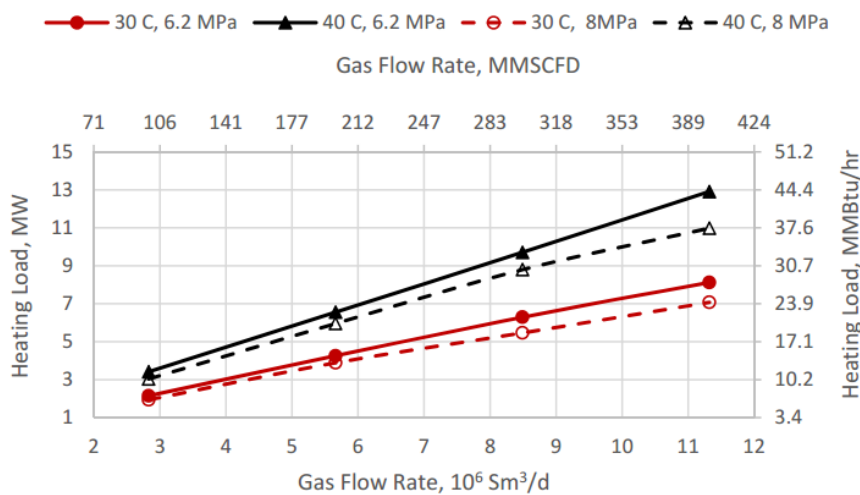


**Figure 35.** Variation of the heating load with the feed gas rate, temperature and pressure.

The different expressions stated in Section 4.3.3 have been calculated for reference conditions of 30 °C and 50 bar. Due to the lack of data and the limitations, several simplifications has been done to obtain the factor:

- The correction factors have been obtained by varying the parameter of interest, while keeping the other at its reference value.
- The heat duty expression due to the feed gas flow rate variation has been obtained at reference conditions.
- The data only takes into account two temperatures and two pressures, therefore the factors' behavior has been assumed linear.
- It can be appreciated from Figure 35 that, with respect to the reference conditions, the heat duty rise at different temperatures and pressures is larger as the gas feed rate increases. This means that the calculated factors are also dependent on the feed gas rate. However, to consider it would have meant an excessive level of complexity that was aimed to avoid.

Therefore, the effect of the gas feed rate on the temperature and pressure correction factors was neglected.



## APPENDIX D: NGL EXTRACTION AND FRACTIONATION

To obtain the de-ethanizer heat duty, a model has been developed to obtain the heat duty as a function of the gas composition. Assuming only C<sub>2+</sub> enters the unit, the heat duty for different compositions has been obtained by using HYSYS.

Equation [D.1] has been defined from the different curves obtained and exposed in Figure 11. The different curves have been approximated to an exponential equation as follows:

$$\dot{q}_{de-ethanizer} \left[ \frac{kWh}{kg} \right] = \alpha * e^{\beta * [C_3]} \quad [D.1]$$

Where  $\dot{q}_{de-ethanizer} [kWh/kg]$  is the specific heat duty of the reboiler per kg of C<sub>2+</sub> entering the de-ethanizer and  $[C_3]$  is the mol fraction of propane.

Afterwards,  $\alpha$  and  $\beta$  have been obtained as a function as a function of the mol fraction of C<sub>2</sub>. Figure 36 presents the variation of  $\alpha$ , that has been approximated to a linear function.

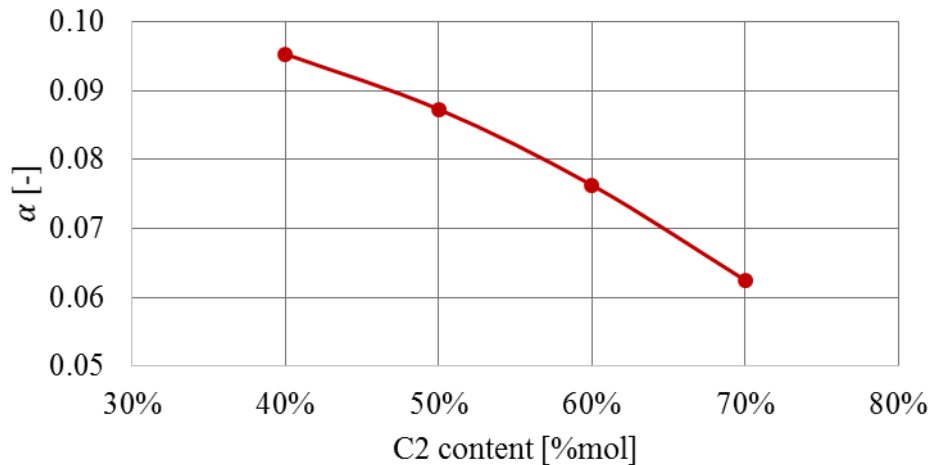


**Figure 36.** Parameter  $\alpha$  as a function of the C<sub>2</sub> mol %.

This approximation to a linear function was a simplification, as it can be seen that the function is not linear, but it was accepted because it did not imply a large deviation in the heat duty estimation.

$$\alpha = -0.11[C_2] + 0.14 \quad [D.2]$$

Figure 37 represents the variation parameter  $\beta$ , that has been approximated to a polynomial function. In this case it was not possible to approximate it to a linear function due to the large deviation it implied.

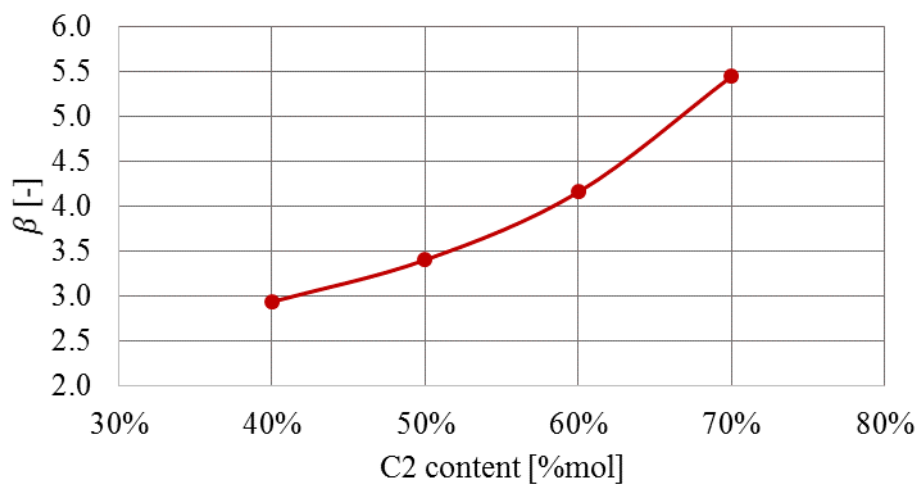


**Figure 37.** Parameter  $\beta$  as a function of the  $C_2$  content.

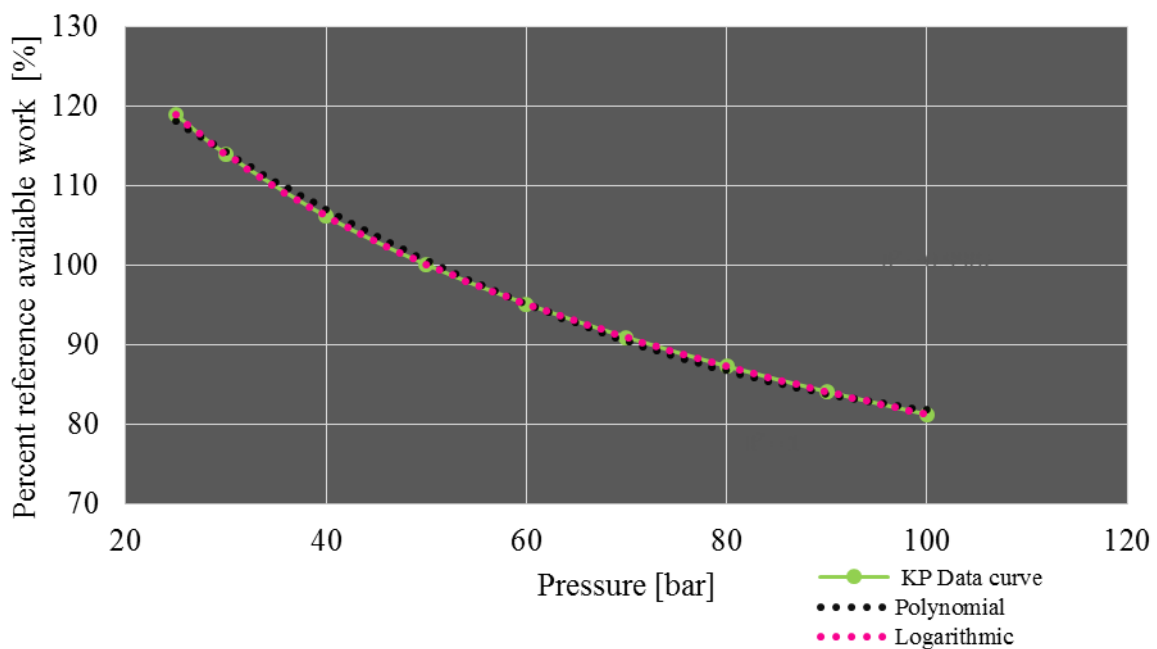
Equation [D.3] defines the polynomial approximation that was used to describe the function obtained.

$$\beta = 20.6[C_2]^2 - 14.3[C_2] + 5.4 \quad [D.3]$$

## APPENDIX E: LIQUEFACTION CORRECTION FACTORS

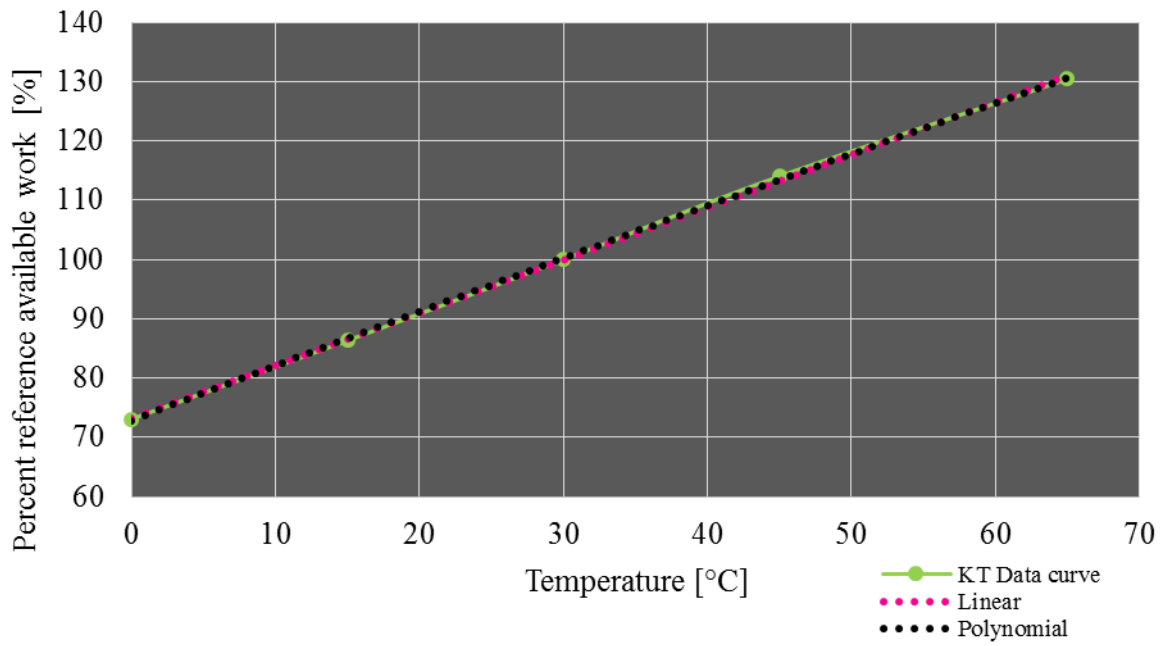
This Appendix presents the different approximations performed for the pressure and temperature correction factors used in the model of the liquefaction unit. The Coefficient of determination  $R^2$  was used to choose the data curve approximation.

Figure 38 presents the two approximations analyzed for  $K_p$ . The  $R^2$  for the polynomial approximation was 0.9982 against 1 for the logarithmic one. Moreover, the logarithmic was preferred due to the simplicity of the expression compared to the polynomial one.



**Figure 38.** Data curve approximations for the definition of  $K_p$ .

Figure 39 shows the two approximations analyzed for  $K_T$ . The  $R^2$  for the polynomial approximations was 0.9997 against the 0.9995 for the linear one. In this case it was decided to use the linear approximation because its accuracy was very high, and the expression was simpler than the polynomial one.



**Figure 39.** Data Curve approximations for the definition of  $K_T$ .

## APPENDIX F: UPSTREAM FUEL GAS INTAKE

This Appendix provides a calculation method that can be implemented on the spreadsheet model in case the upstream fuel gas intake is preferred.

The upstream fuel gas intake assumes that all the fuel gas is taken after the slug catcher. The power consumed by the different processes is a function of the feed gas flow rate. As the fuel gas is directly taken from the feed gas stream, an increase in the power consumption leads to a higher fuel flow rate, and consequently a decrease of the feed gas processed and LNG produced. This fact makes necessary an iterative process for which the Microsoft Excel solver can be used, as well as the formulation of some assumptions.

The composition of the fuel gas is assumed the same as the feed gas stream after the slug catcher, and its GHV is calculated consequently. The fuel gas consumption is assumed to be entirely spent to run the compressors, and the heating needs are assumed to be fully covered by waste heat. Therefore, the heat generation is assumed to be fully covered by the waste heat produced by the gas turbines.

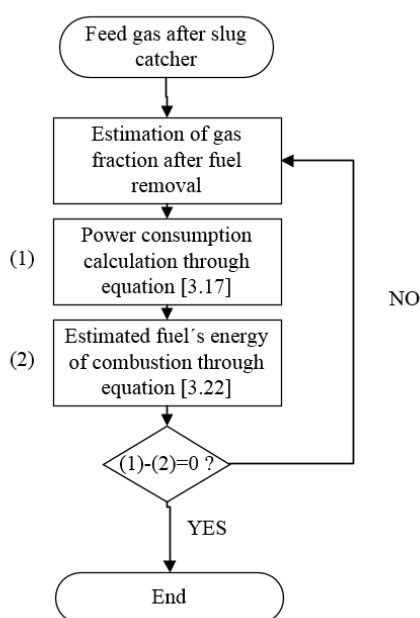


**Figure 40.** Iterative algorithm used to calculate the fuel gas need.

The algorithm gives an estimation of the gas fraction left after the fuel gas removal and obtains the total power consumption through Equation [3.17]. Then, the energy of combustion of the fuel gas obtained is calculated through Equation [3.22] and compared to the previously

calculated total power consumption. The iteration ends once the energy of combustion equals the energy consumption of the entire plant model.

For the implementation of the upstream fuel gas intake model it is necessary to assume that the End flash gas, the BOG and the vapor return from ship are recovered and reliquefied, so the LNG production does not decrease.

## APPENDIX G: NUMERICAL TEST RESULTS

Table 20. Numerical results for the comparison of the six cases.

Parameter	Case A			Case B			Case C		
	Reference	Estimate	Error %	Reference	Estimate	Error %	Reference	Estimate	Error %
Liquefaction power, MW	125	117.4	-6	162	156.2	-4	660	585.7	-3
LNG production, Mtpa	3.3	3	-10	4.2	4.6	10	13.5	13.1	-3
LPG production, Mtpa	0	0	0	0.3	0.25	-16	0	0	0
Condensate production, Mtpa	0.3	0.62	108	0.7	0.72	3	0.3	0.08	-74
CO <sub>2</sub> from feed, tpa	995,000	898,588	-10	640,000	725,906	13	120,000	80,454	-33
CO <sub>2</sub> from liq. drivers, power and heat generation, tpa	797,000	690,563	-13	900,000	732,399	-19	37,000,000	4,245,612	15
Parameter	Case D			Case E			Case F		
	Reference	Estimate	Error %	Reference	Estimate	Error %	Reference	Estimate	Error %
Liquefaction power, MW	124	128.6	4	196	250	28	225	241.7	7
LNG production, Mtpa	3.1	3.2	5	4.1	4.2	2	3.6	3.4	-7
LPG production, Mtpa	0	0	0	0	0	0	0	0	0
Condensate production, Mtpa	0.05	0.19	276	0.01	0.05	410	0.2	0.11	-47
CO <sub>2</sub> from feed, tpa	23,000	0	-	150,000	169,190	13	83,000	83,738	1
CO <sub>2</sub> from liq. drivers, power and heat generation, tpa	820,000	732,422	-11	1,355,000	1,473,602	9	990,000	1,358,925	37

**Table 21.** Numerical results for comparison of cases A and B.

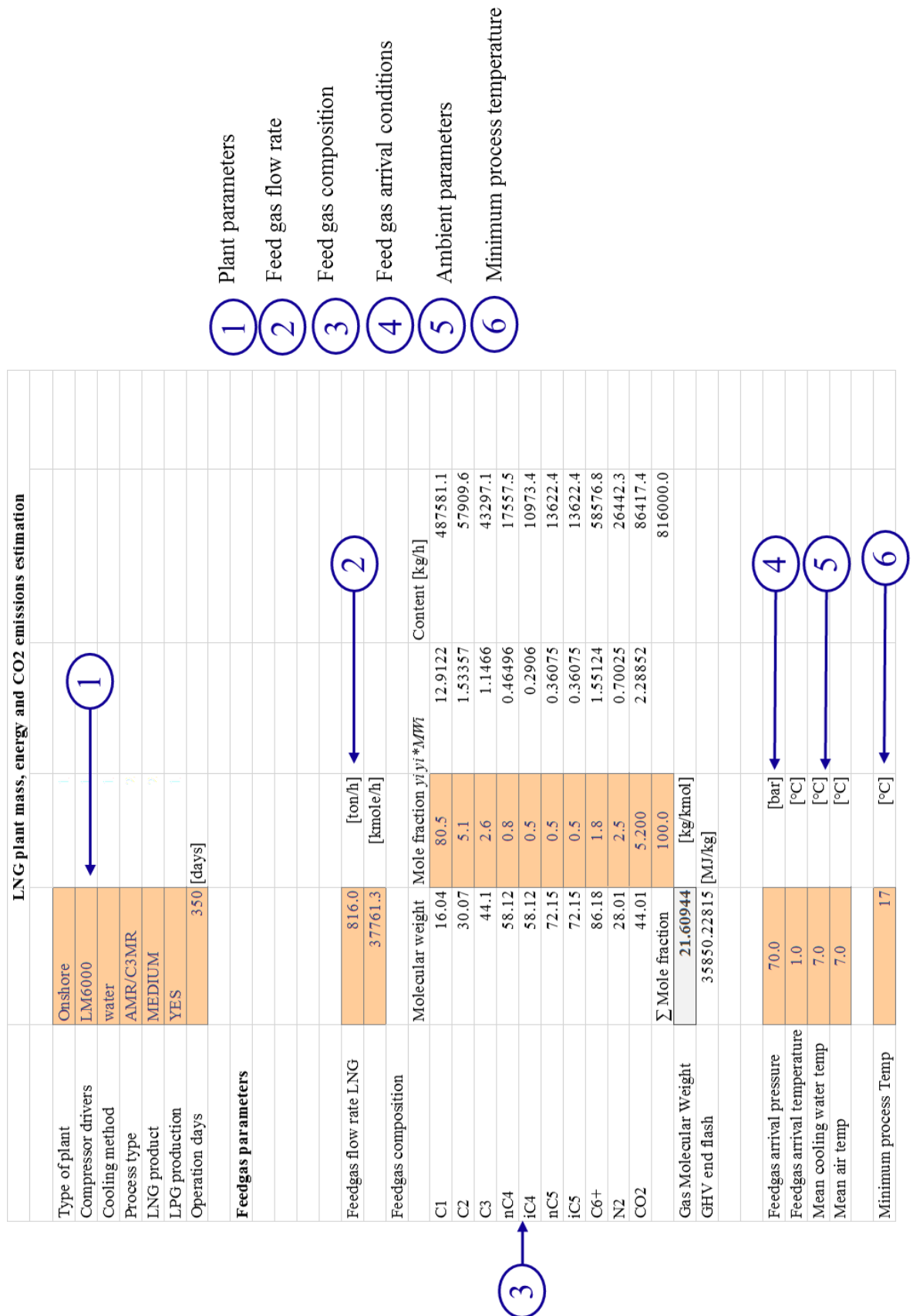
Parameter	Case A			Case B		
	Reference	Estimate	Error %	Reference	Estimate	Error %
Liq. drivers and total electrical power, MW	180.0	159.3	-12.0	218.0	208.4	-4.0
Total heat duty, MW	138.0	143.7	4.0	138.0	132.6	-10.0
MDEA solution regenerator, MW	96.0	98.3	2.0	63.0	74.9	19.0
MDEA solution pump, MW	3.8	5.2	1.0	3.3	4.1	24.0
De-ethanizer, MW	15.5	13.7	-12.0	7.5	31.2	316.0
Dehydration, MW	3.8	7.8	104.0	8.9	4.4	-50.0
Fuel gas flow rate, ton/h	46.8	46.8	11.0	40.0	49.2	23.0
Fuel gas GHV [kJ/kg]	-	37700.0	-	-	35580.0	-



## **APPENDIX H: MODEL IMPLEMENTATION**

Appendix H presents the different sheets contained in the testing model implemented in Microsoft Excel to perform the calculations. As an example, case B is shown. This testing model implemented on Microsoft Excel has been provided together with the report to give an example of how the created model could be implemented on a spreadsheet software.

APPENDICES



- 1 Plant parameters
- 2 Feed gas flow rate
- 3 Feed gas composition
- 4 Feed gas arrival conditions
- 5 Ambient parameters
- 6 Minimum process temperature

Figure 41. Inputs sheet layout.

Gas sweetening unit						
<b>Parameters</b>						
feedgas	3.78E+04 [kmole/hr]					
CO <sub>2</sub>	0.052 [mole fraction]					
Total acid gas feed	1963.586 [kmole/hr]			Regenerator heat duty 74.899035 [MW]		4
				Pumping power 4114.4665 [kW]		
<b>MDEA calculations</b>						
				CO <sub>2</sub> :		
MDEA loading	0.5 [mol/mol]			Removed	8.64E+04 [kg/h]	5
MDEA wt%	50 [%]				7.26E+05 [tpa]	
MDEA MW	119.2 [kg/kmole]					
						1
						2
MDEA flow	3927.173 [kgmole/h]					
MDEA mass flow	468119 [kg/hr]					
Total solution required	936237.9 [kg/hr]					
						3
Excess amine factor	1.2 [-]					
Corrected MDEA required	561742.8 [kg/hr]					
Corrected solution required	1123486 [kg/h]					
						4
						5

CO<sub>2</sub> mole fraction and total acid gas content

MDEA strength and loading

Excess amine factor and corrected MDEA and solution required

MDEA regenerator heat duty and pumping power

CO<sub>2</sub> emissions from the feed gas

Figure 42. Gas Sweetening Unit sheet layout

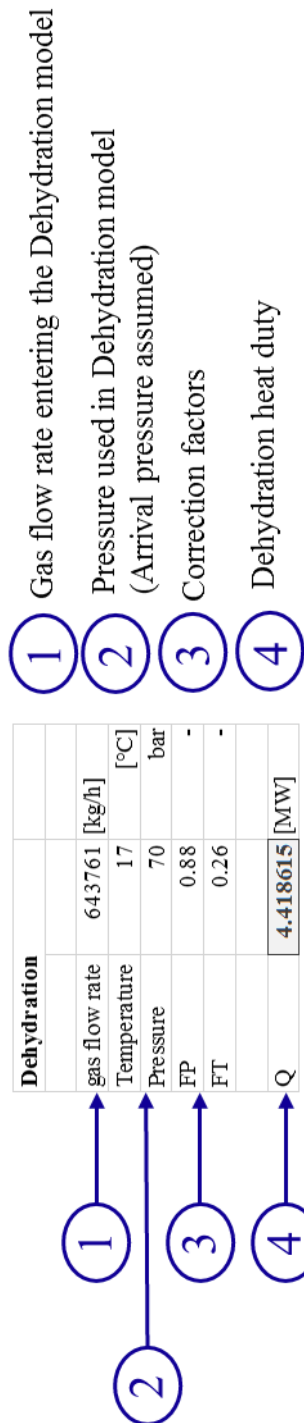


**Figure 43.** Dehydration Unit sheet layout.

Feedgas parameters	NGL extraction									
	Feedgas flow rate 643.7610082 [ton/h]	Mole fraction y <sub>i</sub>	Norm composition	Norm yi*Mwi	Norm Content mol	Norm feedgas mass conten	Norm gas [mole/h]	Gas to liquefaction	Norm gas [mole/h]	Comp gas to liquefaction
Feedgas composition										
	MW [kg/kmol]									
C1	16.04	80.5	0.88	14.04	30397.83	487581.13	30398	487581	30398	0.89
C2	30.07	5.1	0.06	1.67	1925.83	57909.56	1926	57910	1926	0.06
C3	44.1	2.6	0.03	1.25	981.79	43297.08	491	21649	491	0.01
C4	58.12	1.3	0.014	0.82	490.90	28530.91	347	20191	347	0.01
N2	28.01	2.5	0.027	0.76	944.03	26442.33	944	26442	944	0.03
	86.18									
	28.01									
	44.01									
Σ Mole fraction	92.0		1.00	Total	34740.37	643761.01		613772.67	34105.98	1.00
Mean MW	18.5			18.5	[kg/kmol]					

1 Dry gas entering the NGL Extraction model  
 2 Normalized composition at the model inlet  
 3 Flow rate and composition of the gas entering the Liquefaction Unit model. The LNG richness is defined by this composition  
 4 Mean Molecular Weight of the gas entering the NGL Extraction model

Figure 44. NGL Extraction model composition and presentation of the mass flow to liquefaction.

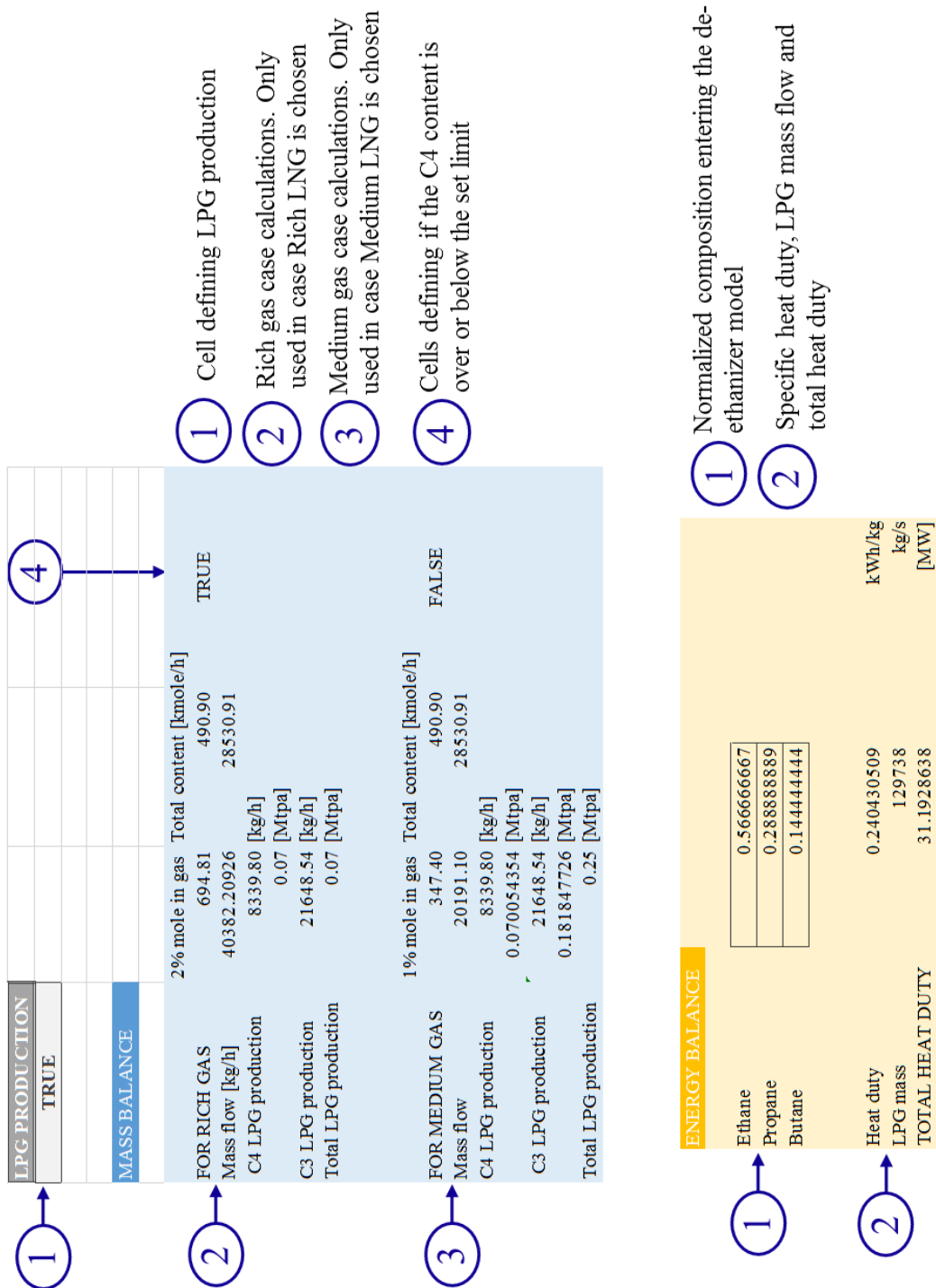


**Figure 45.** These tables present the split ratio contributing to the mass balance of the unit, and the energy balance in the de-ethanizer to obtain the heat duty of the NGL Extraction model.

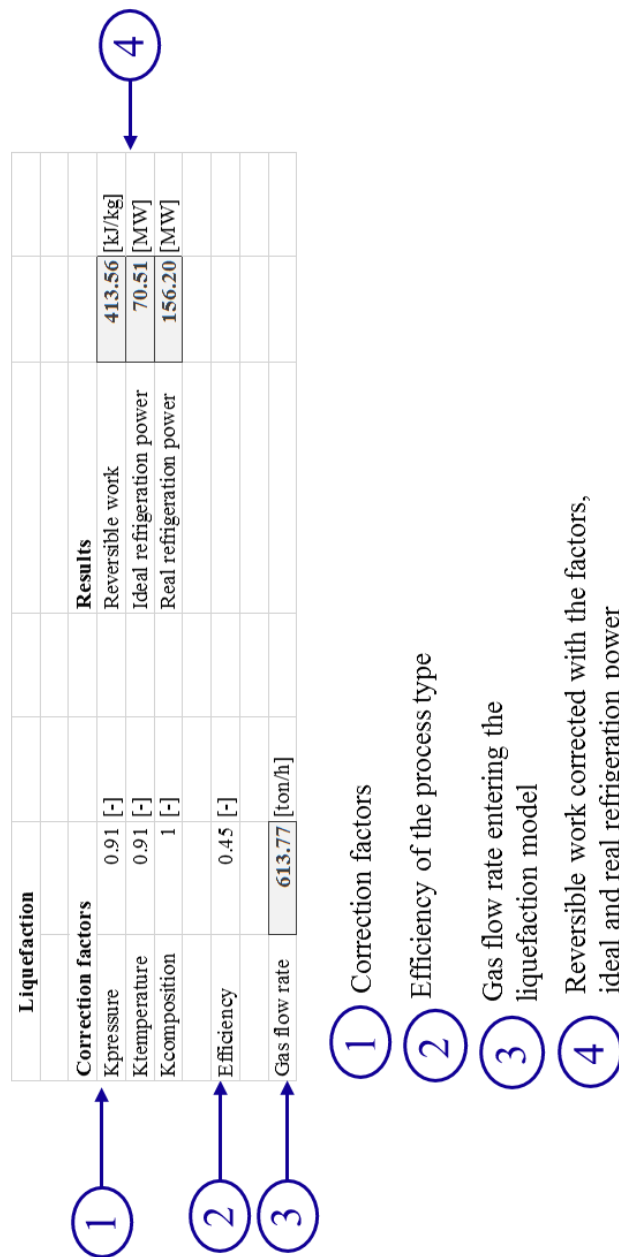
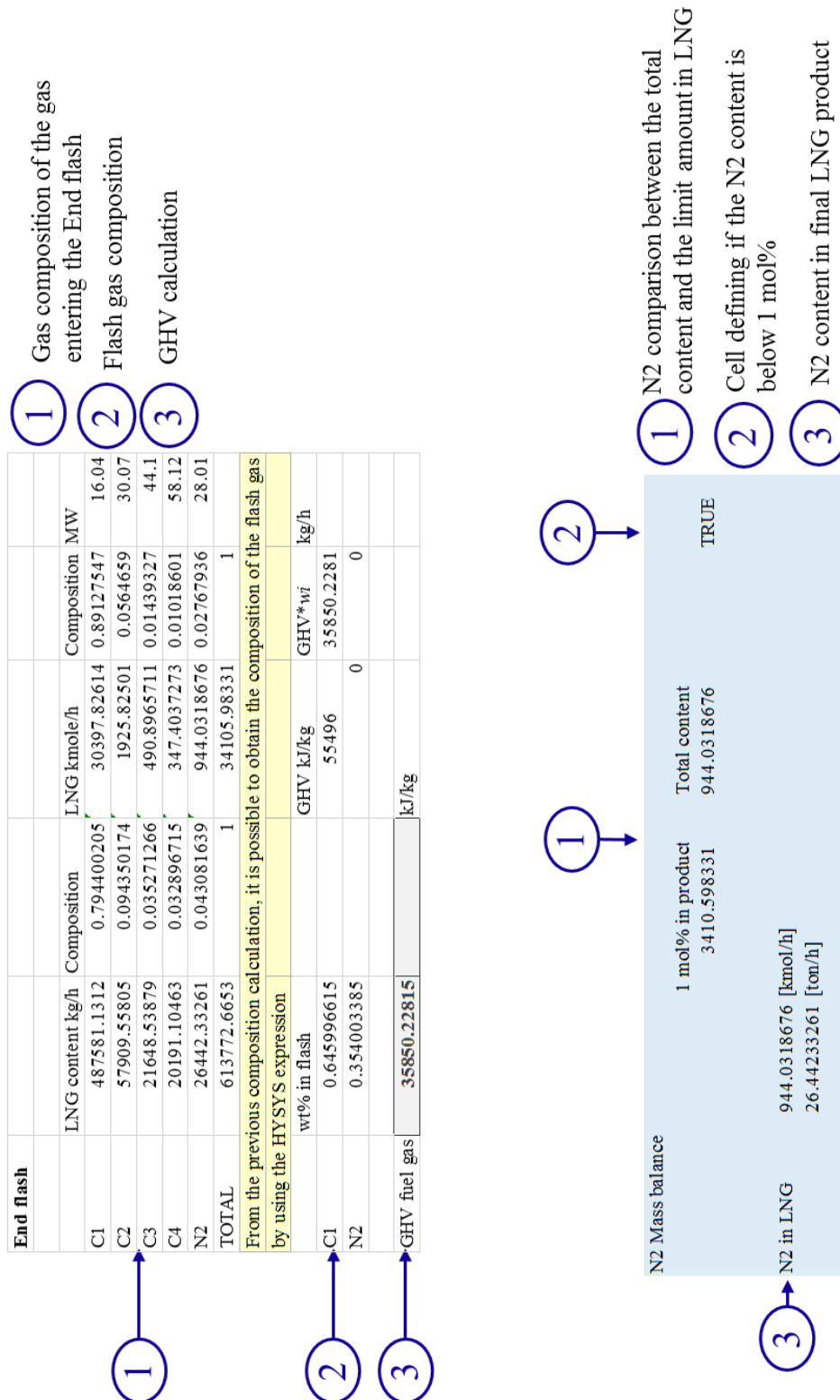


Figure 46. Liquefaction Unit model layout.



**Figure 47.** End flash composition, GHV calculation and split ratio contributing to the mass balance of the model.



Driver									
Design Efficiency		0.38	[-]						
Kefficiency		1.1196	[-]						
Fuel consumption from end flash		13.6643482	[kg/s]						
Fuel percentage of feedgas		49.19165351	[ton/h]						
		6.02838891	[%]						

① Design efficiency of the turbine and correction factor
② Fuel consumption calculation

CO <sub>2</sub> emission									
Mass fraction y <sub>i</sub>	Mass content [kg/h]	Mol Content [kmol/h]	Mole fraction	CO <sub>2</sub> produced [kmol/h]					
C1	0.645996615	31.77764166	1981.149729	0.761144377	1981.149729				
N2	0.354003385	17.41401185	621.7069565	0.238855623	621.7069565				
			1		2602.856686				
Total CO <sub>2</sub> produced	1981.149729	kg/h	87190.39958	tpa	732399.3565				

① Fuel gas composition and CO<sub>2</sub> generation
② Total CO<sub>2</sub> emissions

**Figure 48.** Driver model sheet layout and CO<sub>2</sub> emissions estimation from the liquefaction drivers, electrical power consumption and heat generation.

<b>Results</b>			
<b>Overall results</b>			
<b>Electrical power and heat balance</b>			
Total compressor power	208.4	[MW]	
Heat duty	132.6	[MW]	
Liquefaction power	156.2	[MW]	
Specific liquefaction power	276.7	[kWh/ton LNG]	
CO <sub>2</sub> solution regenerator	74.9	[MW]	
CO <sub>2</sub> Solution pump	4.1	[MW]	
De-ethanizer	31.2	[MW]	
Dehydration	4.4	[MW]	
<b>Mass balance</b>			
CO <sub>2</sub> from feed	725906.4	[tpa]	
CO <sub>2</sub> from drivers and power/heat gen	732399.4	[tpa]	
LNG production	4.7	[Mtpa]	
LPG production	0.25	[Mtpa]	
Condensate production	0.72	[Mtpa]	
Fuel gas flow rate	49.2	[ton/h]	

**Figure 49.** Results sheet summary presenting all the results estimated.